



Characteristics and Physics of Plasma Detachment in the Plume of the VASIMR[®] VX-200 Engine

By

Christopher S. Olsen, Ph.D

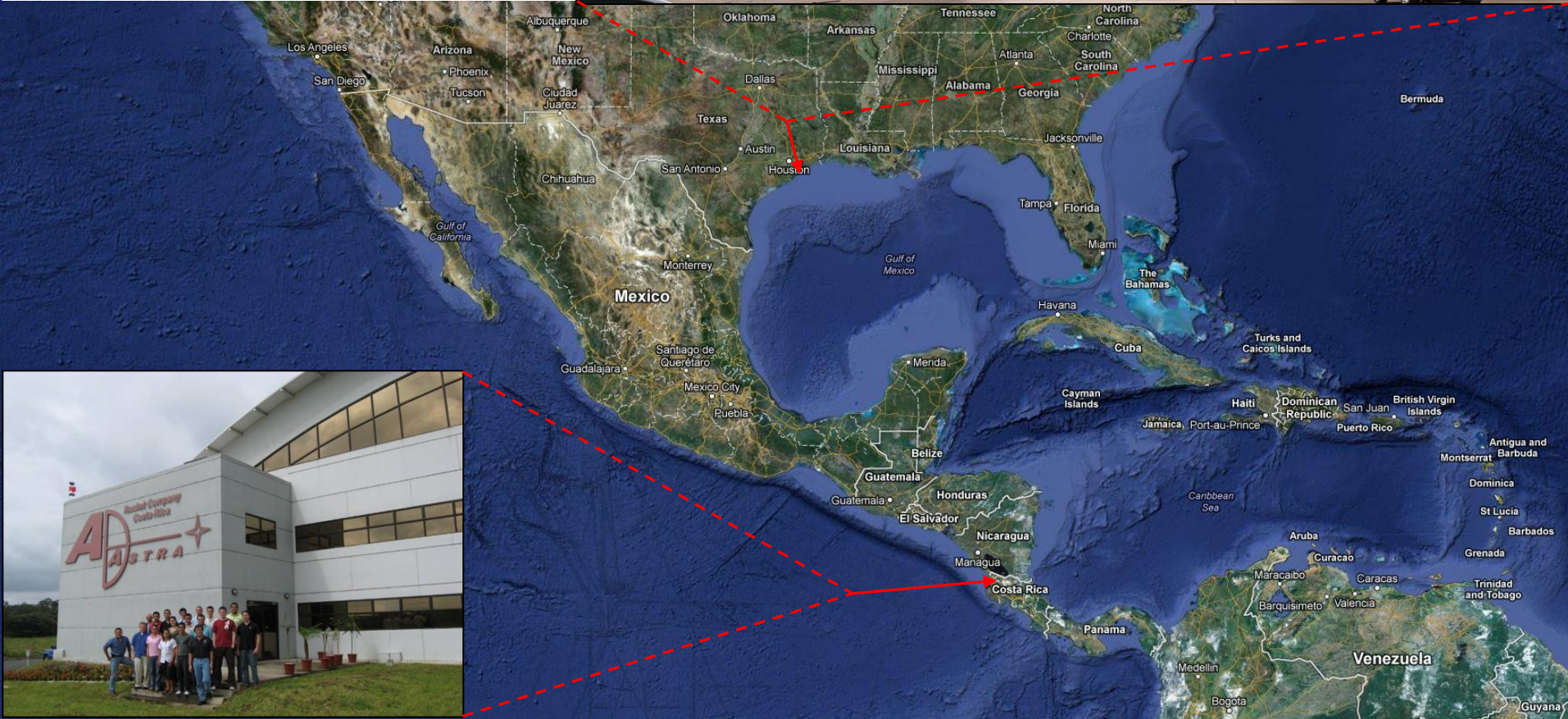
**Senior Research Scientist / Laboratory Operations Manager
Ad Astra Rocket Company**

**Space Physics Seminar at the University of Houston at Clear Lake
April 18, 2013
Bayou 1218**

Ad Astra Rocket Company...Who are we?

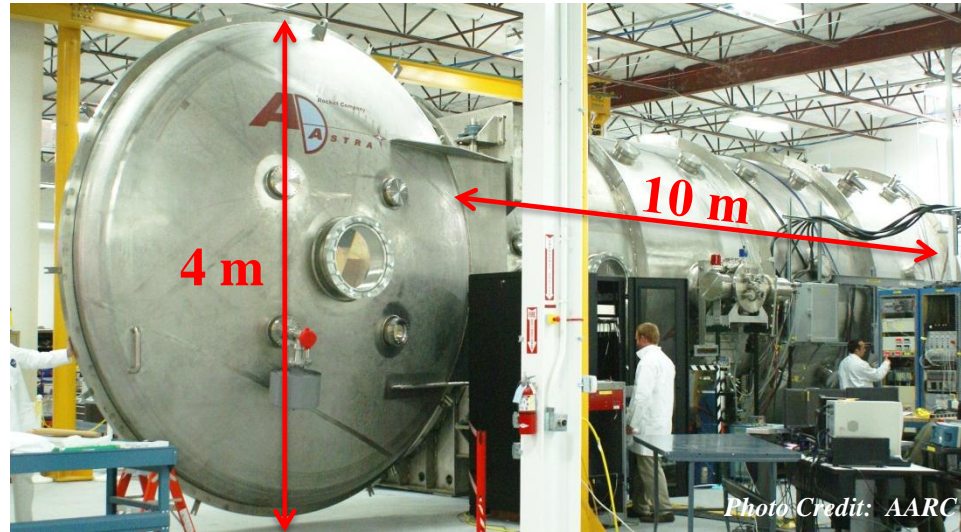
The Ad Astra Rocket Company has two facilities that primarily deal with the testing, design, and fabrication of the VASIMR[®] engine. We are also involved in studying more efficient uses and implementations of renewable energy.

Webster, Texas Laboratory (25,000 ft²)

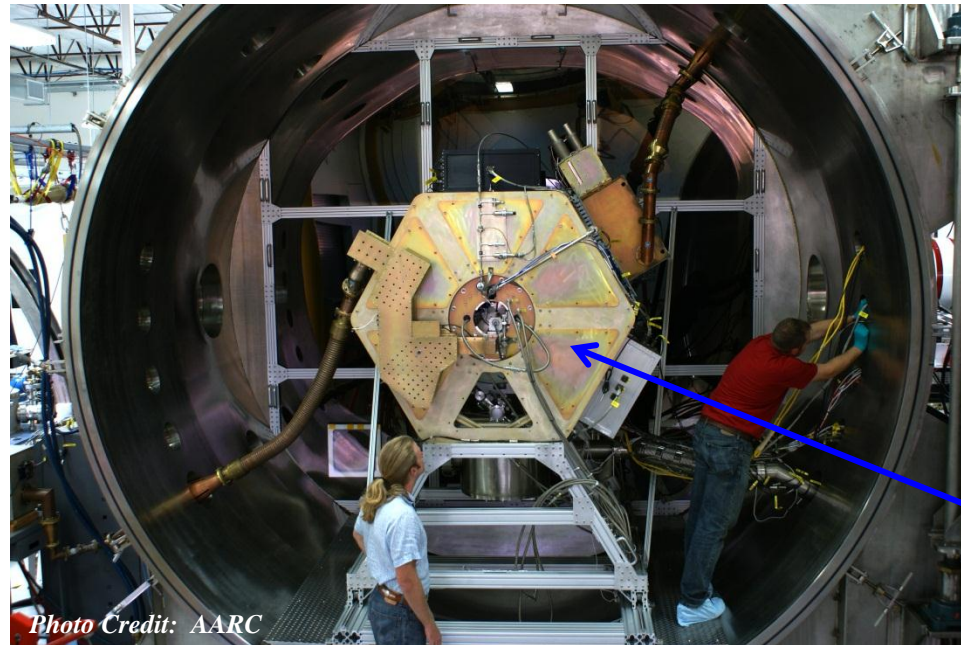


Liberia, Guanacaste, Costa Rica

VASIMR® Test Facility

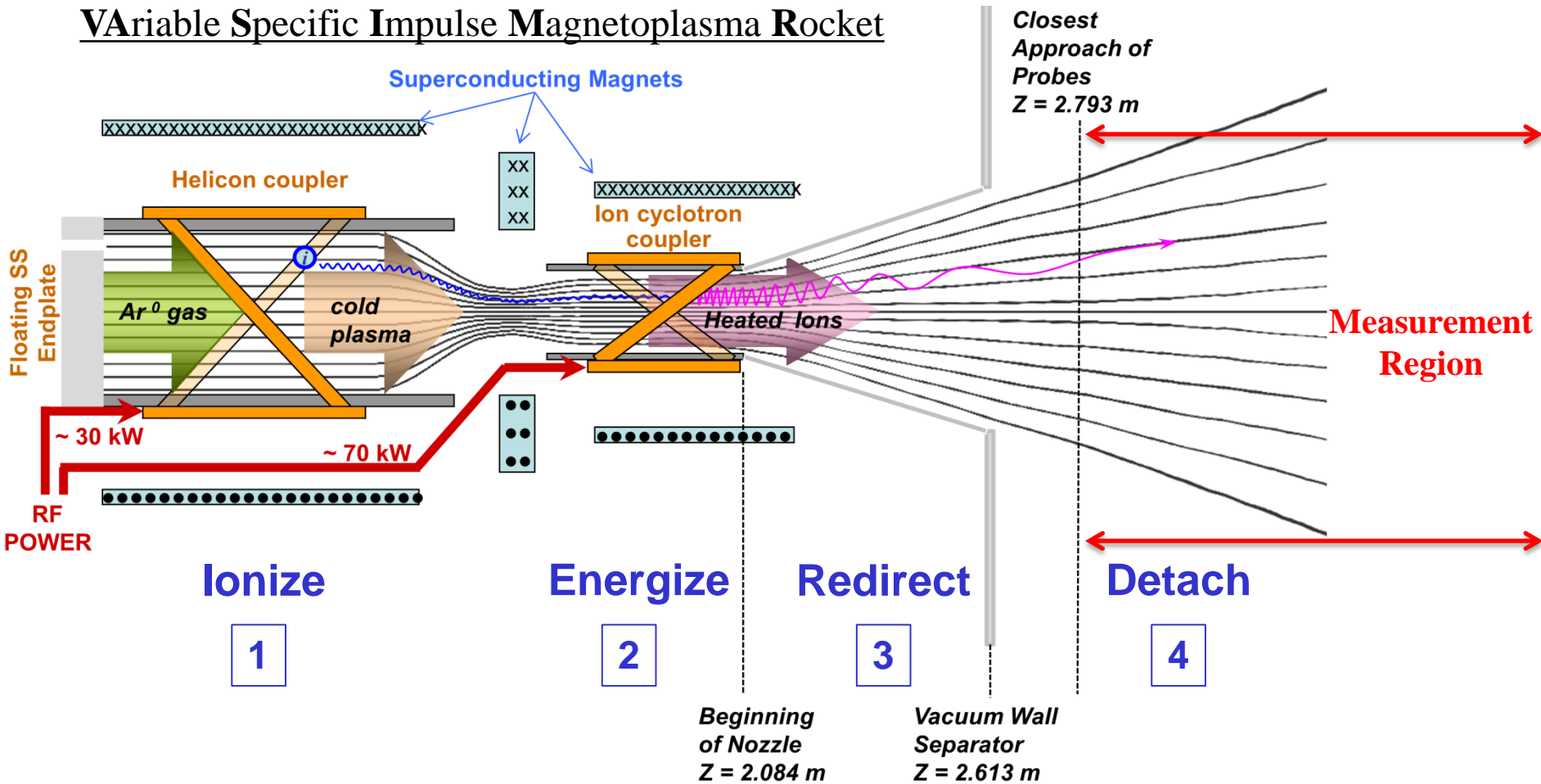


- Located in Webster, Texas
- VASIMR® test bed operated within a 150 m³ vacuum chamber.
- VASIMR® is capable of throttling power ranging from 10 kW – 220 kW corresponding to less than 1000 s to greater than 5000 s I_{sp} for argon.
- Peak magnetic field strengths greater than 2 T and nozzle field drop-off spans over 3 orders of magnitude.
- Liquid nitrogen assisted cryopanel enable pumping speeds of nearly 250,000 liters/s and base pressures below 10⁻⁸ torr.
- Fiber optic transmission and FPGA control permit steady state plasma operation within 50 ms allowing data to be taken when charge-exchange effects are minimal.



VX-200

Variable Specific Impulse Magnetoplasma Rocket



1. Helicon ionizes propellant gas forming cold plasma
2. Ion energy is boosted through Ion Cyclotron Resonance/Heating (ICH)
3. Magnetic nozzle converts perpendicular motion into parallel flow
4. Plasma detaches from the nozzle magnetic field

VX-200 Firing at 200 kW



VX200 at 200kW

(Graphite Glowing at ~ 1200° C)

Plasma Detachment Problem

- Understanding plasma confinement, cross-field transport, and demagnetization are important to the fields of astrophysics and plasma physics
- A medium that utilizes each of these processes are magnetic nozzles
- Similar to Laval Nozzles, magnetic nozzles may be used to convert or redirect the motion of charged particles into vectored thrust
- Unlike Laval nozzles, the charged particles are inherently attached to the magnetic nozzle and must separate in order to produce net thrust
- Understanding the mechanisms and processes that permit plasma to separate from the field lines is known as the plasma detachment problem

Applications or Observed Phenomena

- Jets from Stars/Active Galactic Nuclei
- Stellar Wind/Solar Atmosphere/Merging Sunspots
- Earth magnetosphere/Aurorae
- Electric Propulsion
- Plasma Processing/Fusion Research

Research Objective/Proposal

- Use the plume of the VASIMR[®] VX-200 to experimentally measure detached plasma
- Characterize the detachment process and verify theories consistent with the data

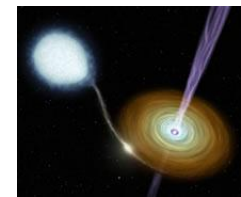
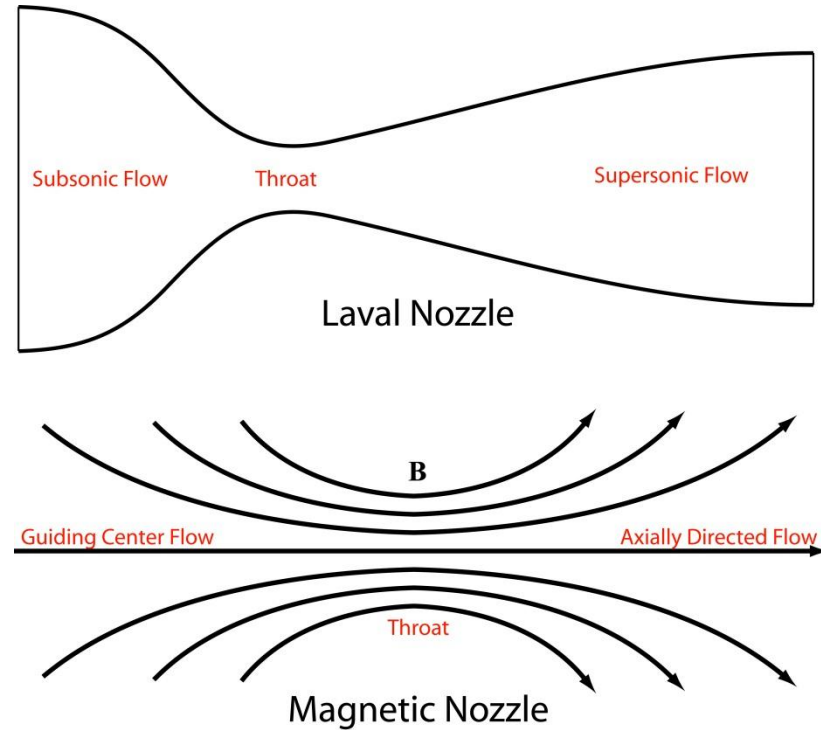


Photo Credit: NASA

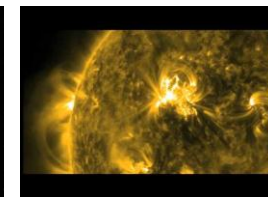


Photo Credit: NASA

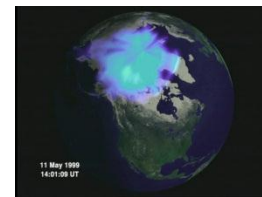


Photo Credit: NASA



Photo Credit: AARC

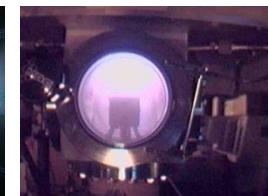


Photo Credit: CeMOS

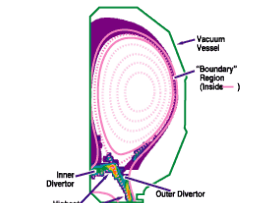


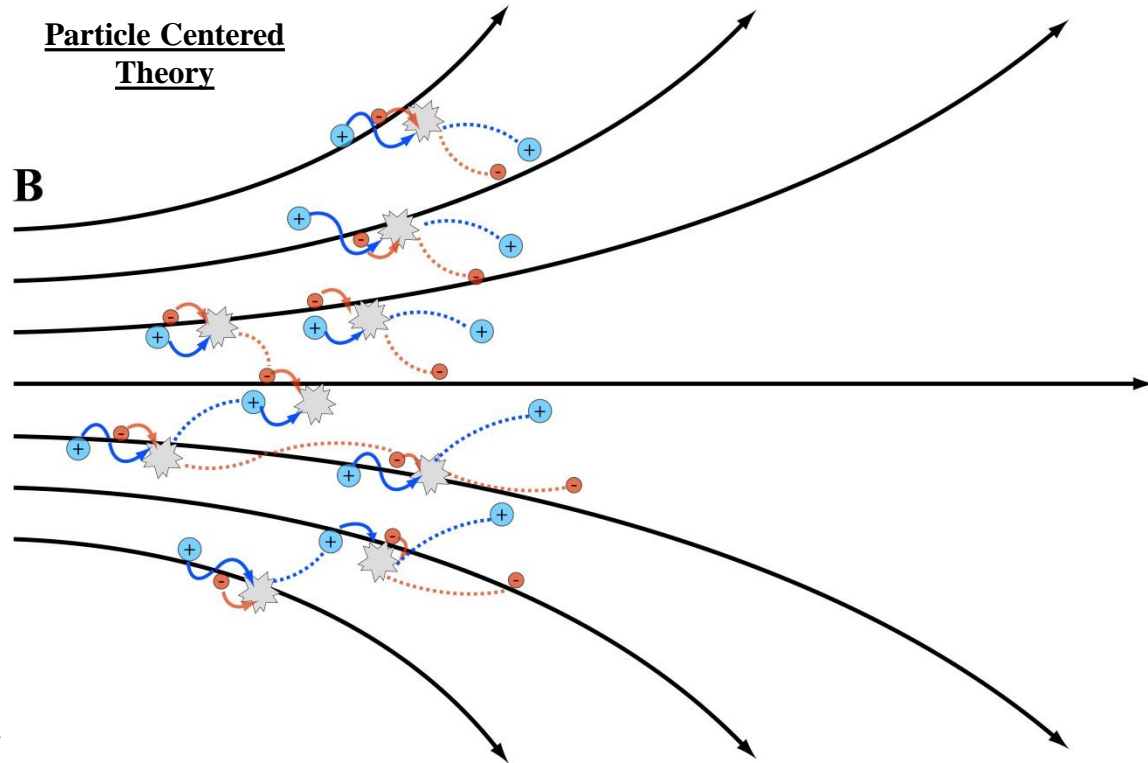
Photo Credit: ITER

Currently proposed theories for detachment

- Collisional Detachment Mechanisms:
 - Electron – Ion Recombination —————→ **Too Slow!**
 - Resistive Diffusion —————→ **Occurring, but not enough**
- Collisionless Detachment Mechanisms:
 - Preservation of the Frozen-In Condition
 - MHD Field Line Stretching —————→ **Not observed**
 - Magnetic Reconnection —————→ **Not observed**
 - Loss of Adiabaticity ←———— **Happening for ions and presumably electrons**
 - Weakly Magnetized Ions and variants of electron inertia
 - Electron Inertia —————→ **Does not align with data**
 - Electron Inertia w/ Rotation —————→ **Unrealistic conditions**
 - Electron Inertia w/ Current Closure —————→ **Not observed**
 - Plasma Turbulence and Anomalous Resistivity ←————
Enhances electron cross-field transport

Current Theory: Resistive Diffusion

- A form of collision-based detachment that involves electrons and/or ions resistively diffusing across the nozzle magnetic field
- Supporters of this type of detachment have been Chubb (1971), Gerwin (1990), Moses (1992), and York (1992) usually involving high plasma densities
- Classical collisional diffusion is governed by Fick's law where a flux of particles diffuse down a density gradient
- The cross-field diffusion coefficient, D_{\perp} , depends on the collision frequency and location in the nozzle field and is related to the mobility
- The cross field particle velocity may also include electric field, $E \times B$, and diamagnetic drift terms
- Many experiments will follow Bohm diffusion proportional to $1/B$, but α ($\sim 1/16$) must be experimentally verified



Fick's Law: $\Gamma = -D\nabla n$

Cross-Field Diffusion Coefficient: $D_{\perp} = \frac{kT}{mv_m} \frac{1}{1 + (\Omega_c \tau_m)^2} = \mu T$

Cross Field Velocity: $u_{\perp} = \pm \mu_{\perp} E - D_{\perp} \frac{\nabla n}{n} + \frac{u_E + u_D}{1 + (\Omega_c \tau_m)^{-2}}$

Bohm Diffusion Coefficient: $D_B = \alpha \frac{T_e}{B}$

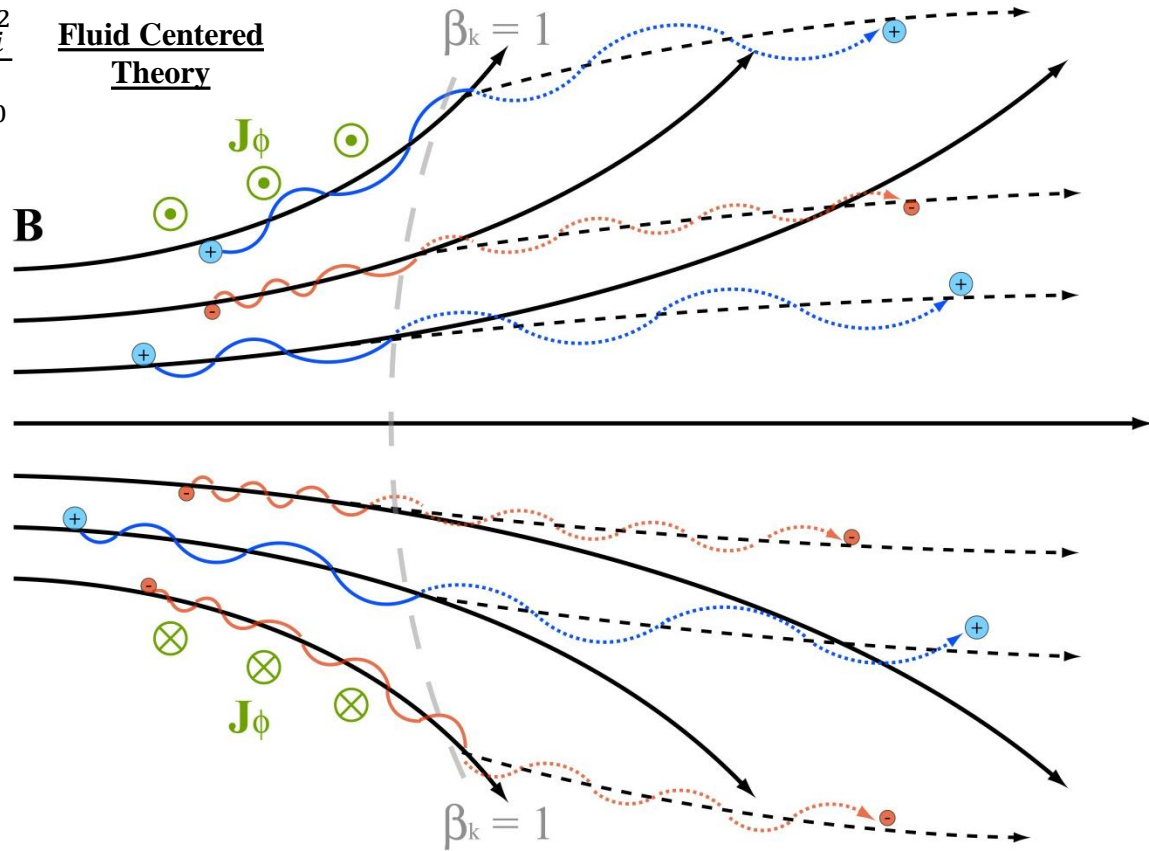
Is Bohm diffusion ($\alpha \sim 1/16$) enough for detachment?

Current Theory: MHD Line Stretching

Plasma Kinetic Beta: $\beta_k = \left(\frac{v}{v_A}\right)^2 = \frac{nM_i u_i^2}{B^2/\mu_0}$

Fluid Centered Theory

$\beta_k = 1$



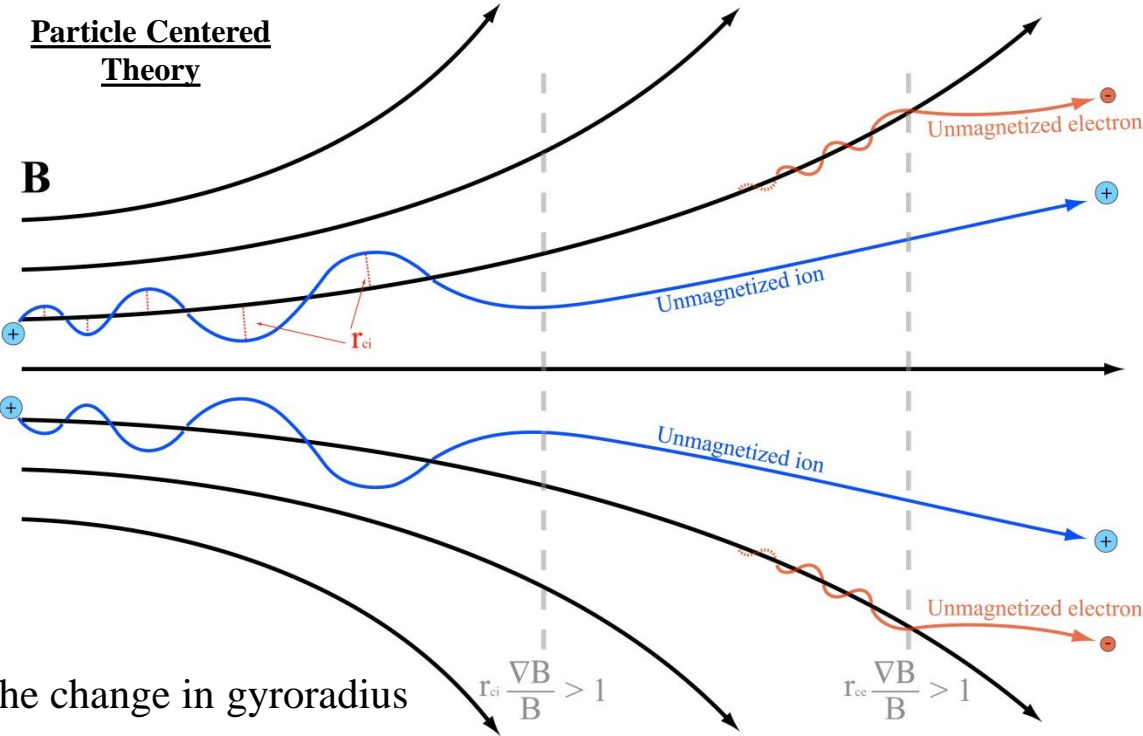
- The MHD Detachment scenario involving super-Alfvénic plasma flow stretching B field lines was suggested as far back as 1958 (E. Parker)
- This detachment concept was applied to magnetic nozzles in a more mathematically rigorous treatment by Arefiev and Breizman (2005)
- They applied an ideal MHD basis to a cold plasma
- The expanding flow created azimuthal currents enabling the field lines to stretch out to infinity
- Small perturbations cause a rarefaction layer to form along the edge
- Magnetic flux outside this edge drops to zero
- The plasma flow carries the magnetic flux effectively preserving the frozen-in condition

Steady-state magnetic field across the nozzle from a Super-Alfvénic plasma flow

$$B(r, z) = \begin{cases} \frac{2\Phi_0}{z^2\theta_0^2}, & r \leq r_{rw} \\ B_0 \frac{z_0^2 v^2}{z^2 9v_A^2} \left[1 - \frac{z_0}{z}\right]^{-2} \left[\frac{r}{z} - \theta_0 - \frac{2v_A}{v} \left(1 - \frac{z_0}{z}\right)\right]^2, & r_{rw} < r < r_{pv} \\ 0, & r_{pv} \leq r \end{cases}$$

Current Theory: Loss of Adiabatic Invariant

- Detachment occurs from the breakdown of the first adiabatic invariant or magnetic moment
- Supporters include Kosmahl (1967), Carter (1999), Ilin (2002), Gesto (2006), Colleti (2007), Little (2010), and Terasaka (2010)
- The magnetic nozzle converts perpendicular velocity into parallel velocity while μ is still conserved
- The action integral from Faraday's law breaks down when the particles gyro-orbit becomes too eccentric
- This demagnetization will occur when the change in gyroradius becomes comparable to itself
- This condition may be expressed in terms of the path length and change in gyrofrequency



Conservation of Magnetic Moment

$$\mu = \pi r_c^2 \cdot \frac{q\Omega_c}{2\pi} = \frac{1}{2} m v^2$$

$$\frac{v_{\perp i}^2 + v_{\parallel i}^2}{B_i} = \frac{v_{\perp f}^2 + v_{\parallel f}^2}{B_f}$$

Variable B field causes the gyro-orbit to become eccentric:

$$\Rightarrow \oint E \cdot ds \neq - \int \frac{dB}{dt} \cdot dS$$

The change in gyroradius can be expressed as:

$$\frac{\Delta r_c}{r_c} = \left[\frac{\Delta \mu}{2\mu} - \frac{\Delta \Omega_c}{\Omega_c} \right] \approx - \frac{\Delta \Omega_c}{\Omega_c} \geq 1$$

The change in gyrofrequency...

$$\frac{\Delta \Omega_c}{\Omega_c} \approx \Delta s \hat{b} \cdot \frac{|\nabla B|}{B}$$

and path length ...

$$\Delta s \approx \frac{2\pi v}{\langle \Omega_c \rangle} = \frac{v}{\langle f_c \rangle}$$

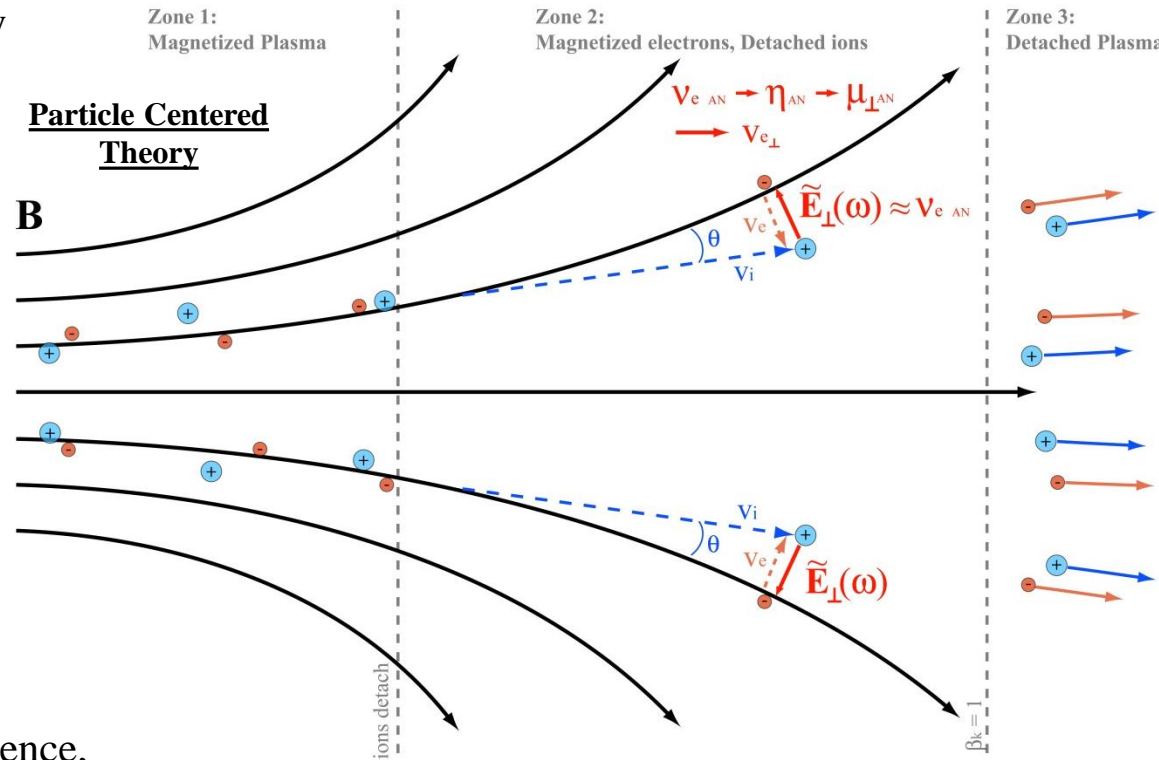
lead to the ...

Detachment Condition:

$$\frac{v}{\langle f_c \rangle} \frac{|\nabla B|}{B} = r_c \frac{|\nabla B|}{B} \cong 1$$

Current Theory: Plasma Turbulence

- Anomalous resistivity may be driven by turbulence brought about by plasma instabilities
- Hurtig and Brenning (2005) of KTH have shown the in phase correlation between electron density and electric field fluctuations postulating that the instability driving this turbulence is a form of the Modified Two-Stream Instability (MTSI).
- The lower hybrid drift instability (LHDI) is a fluidlike, T_e/T_i dependent version of the MTSI with characteristic frequencies comparable to the lower hybrid frequency.
- The effective collision frequency, and hence, resistance/mobility is enhanced
- A force balance will determine the overall response to the transport
- This enhanced transport may enable detachment so long as the cross-field velocity can approximate the ion velocity so as to mitigate space-charge effects



Effective Resistivity:

$$\eta_{eff} = \eta_c + \eta_{AN} \approx \eta_c + \frac{\langle \tilde{n}_e \tilde{E} \rangle}{qv_{de} \langle \tilde{n}_e \rangle^2}$$

Effective Momentum Transfer Time:

$$\tau_{eff} = \frac{m_e}{\eta_{eff} q^2 n_e}$$

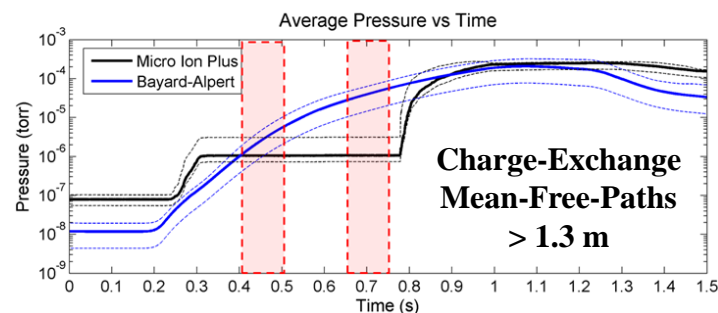
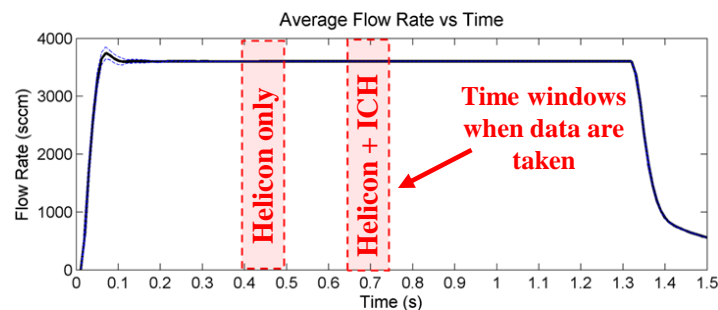
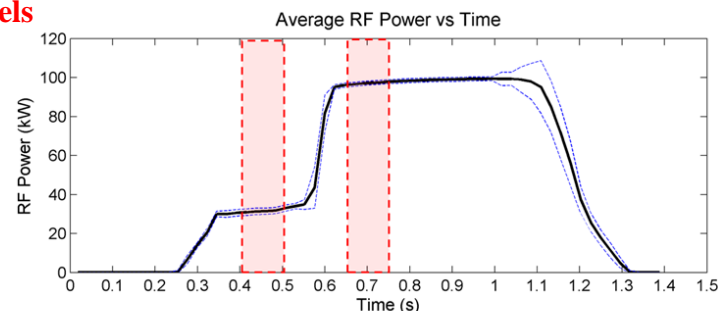
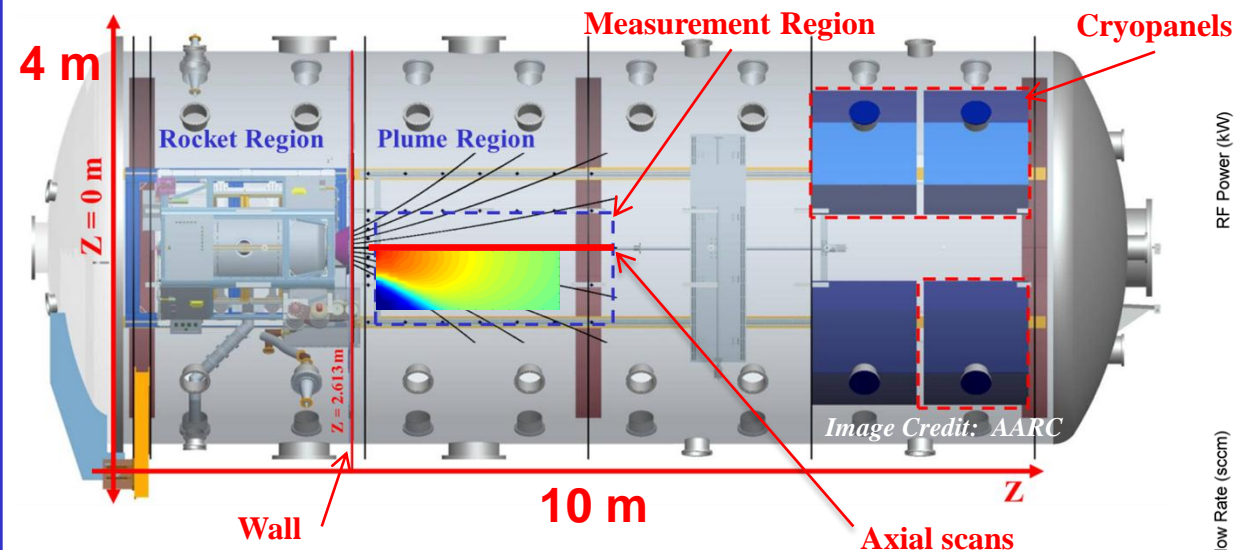
Enhanced cross field mobility:

$$\mu_\perp = \frac{1}{B} \left[\frac{\Omega_c \tau_{eff}}{1 + \Omega_c^2 \tau_{eff}^2} \right]$$

MTSI Dispersion Relation:

$$1 + \frac{k_z^2 \omega_{pe}^2}{k^2 \Omega_e^2} - \frac{\omega_{pi}^2}{(\omega - k_z v_{de})^2} - \frac{k_y^2 \omega_{pe}^2}{k^2 \omega^2} = 0$$

Experiment/Facility Setup



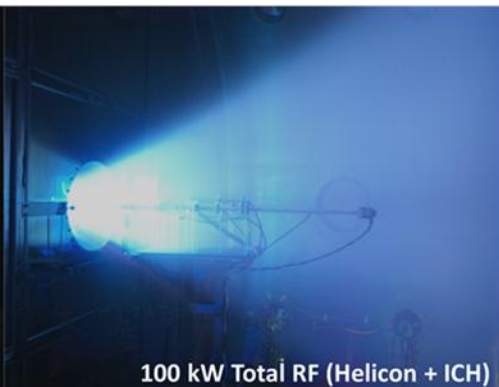
Parameter/Setpoint	Experiment Values
Gas Species	Argon (99.999%)
Flow Rate	107.28 +/- 0.015 mg/s
Plasma Source Power (Helicon RF)	31.1 +/- 0.7 kW
Plasma Heating Power (ICH RF)	68.9 +/- 0.9 kW
Helicon Wave Frequency	6.78 MHz
Peak Magnetic Field Strength	> 2 T
Measured Nozzle Field Strength (on axis)	10 - 740 G
Ion Energy	50 - 280 eV
# of Shots per mapping	91, 450, 1104
Shot Duration	2 s
Helicon Data Window	0.4 - 0.5 s
ICH Data Window	0.65 - 0.75 s
Chamber Volume	150 m ³
Chamber Background Pressure	10 ⁻⁸ - 10 ⁻⁴ torr
Charge Exchange mean free path (Helicon)	12.6 - 78.1 m
Charge Exchange mean free path (ICH)	1.3 - 3.2 m
Argon Pumping Speed	188,000 liters/s

Typical RF Power, Gas Flow and Pressure Rise during a single firing. Solid lines are averages over 450 firings. Dashed lines bound values to one standard deviation.

**Power setting during
data window #1:
Lower momentum
13 – 17 km/s
30 kW**



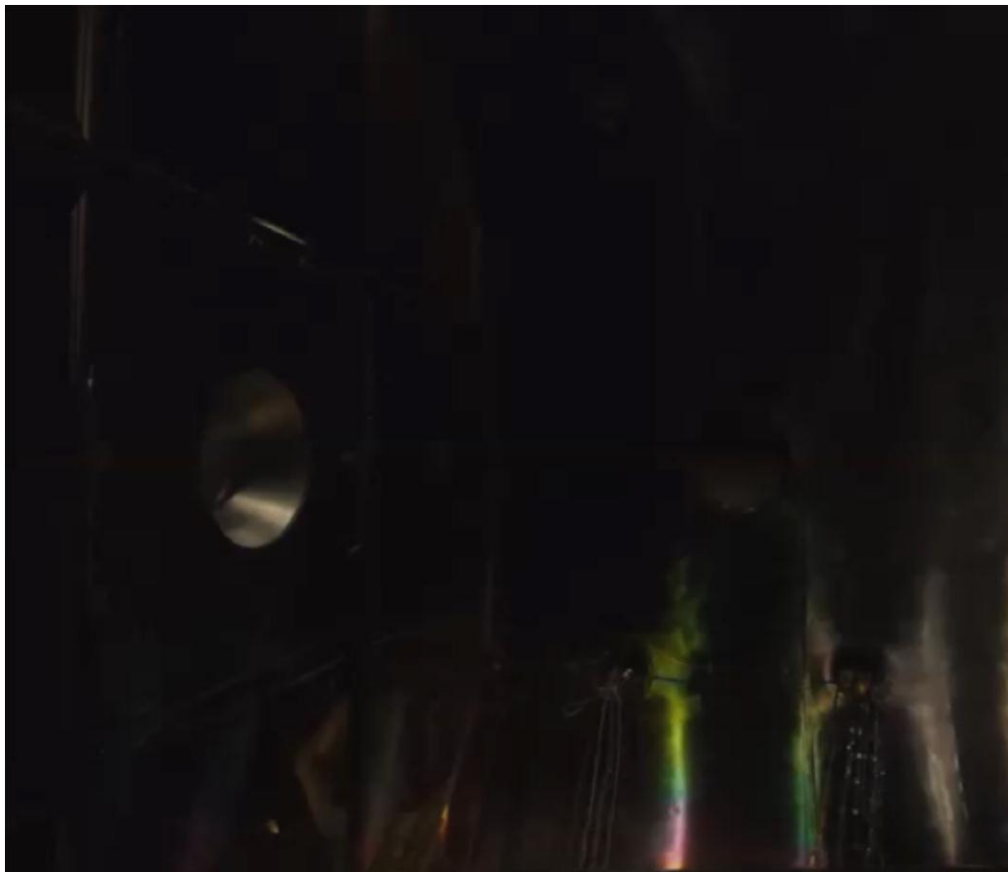
30 kW Helicon

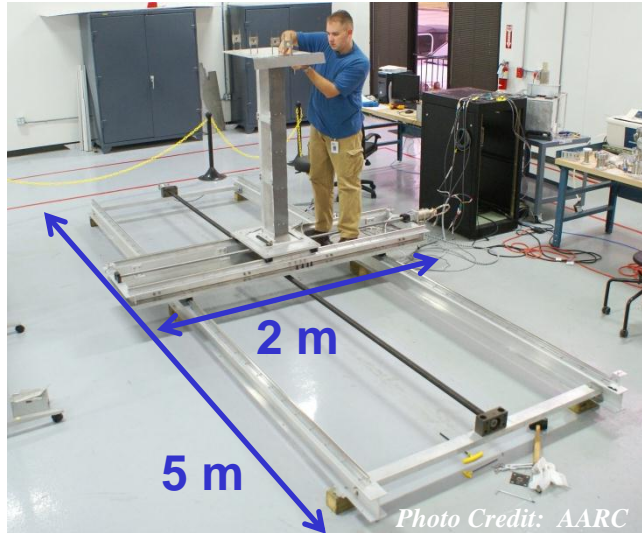


100 kW Total RF (Helicon + ICH)

**Power setting during
data window #2:
Higher momentum
27 – 31 km/s
100 kW**

**VX-200
Firing at
 $P_{RF} = 100 \text{ kW}$
for 10 s**





Translation Stage during testing/assembly

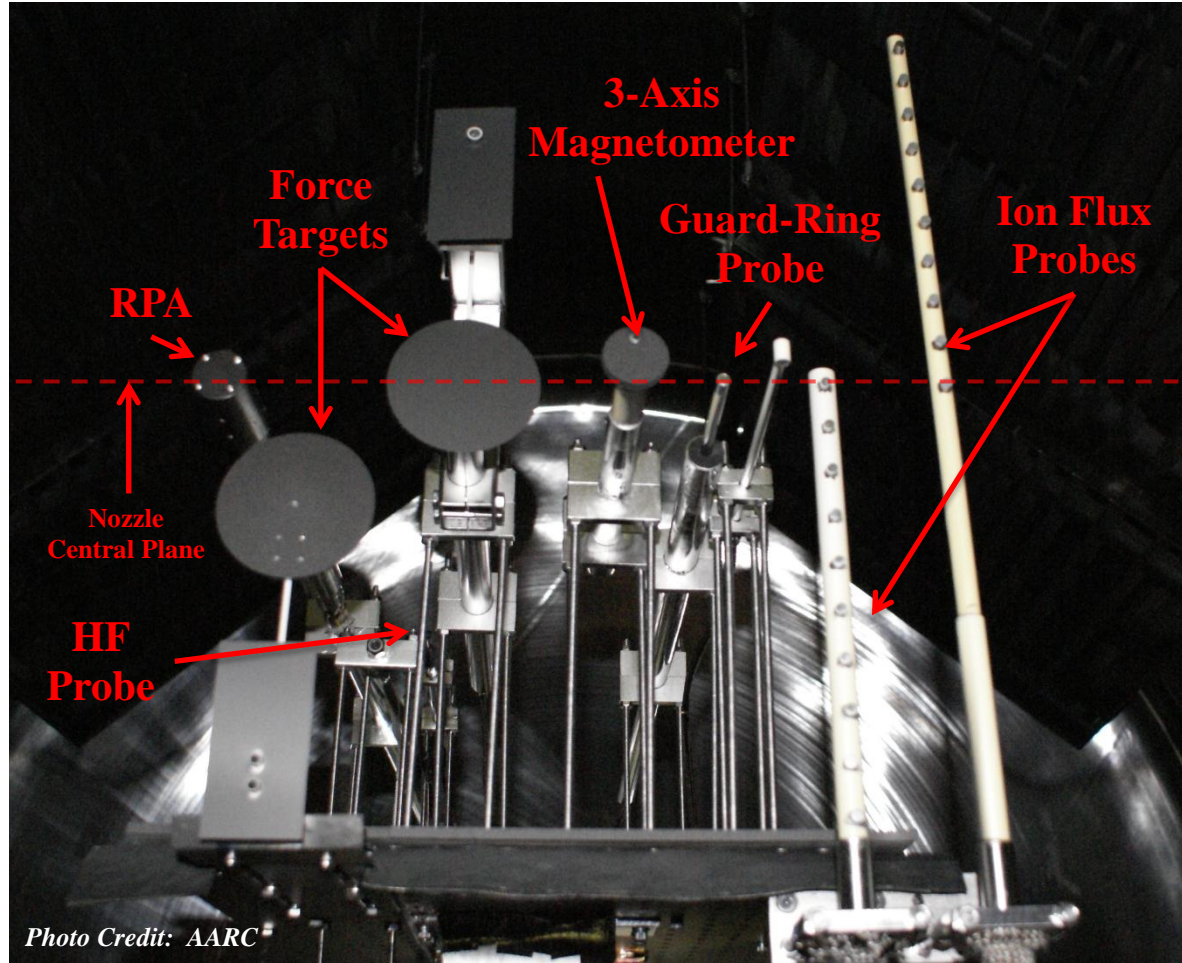
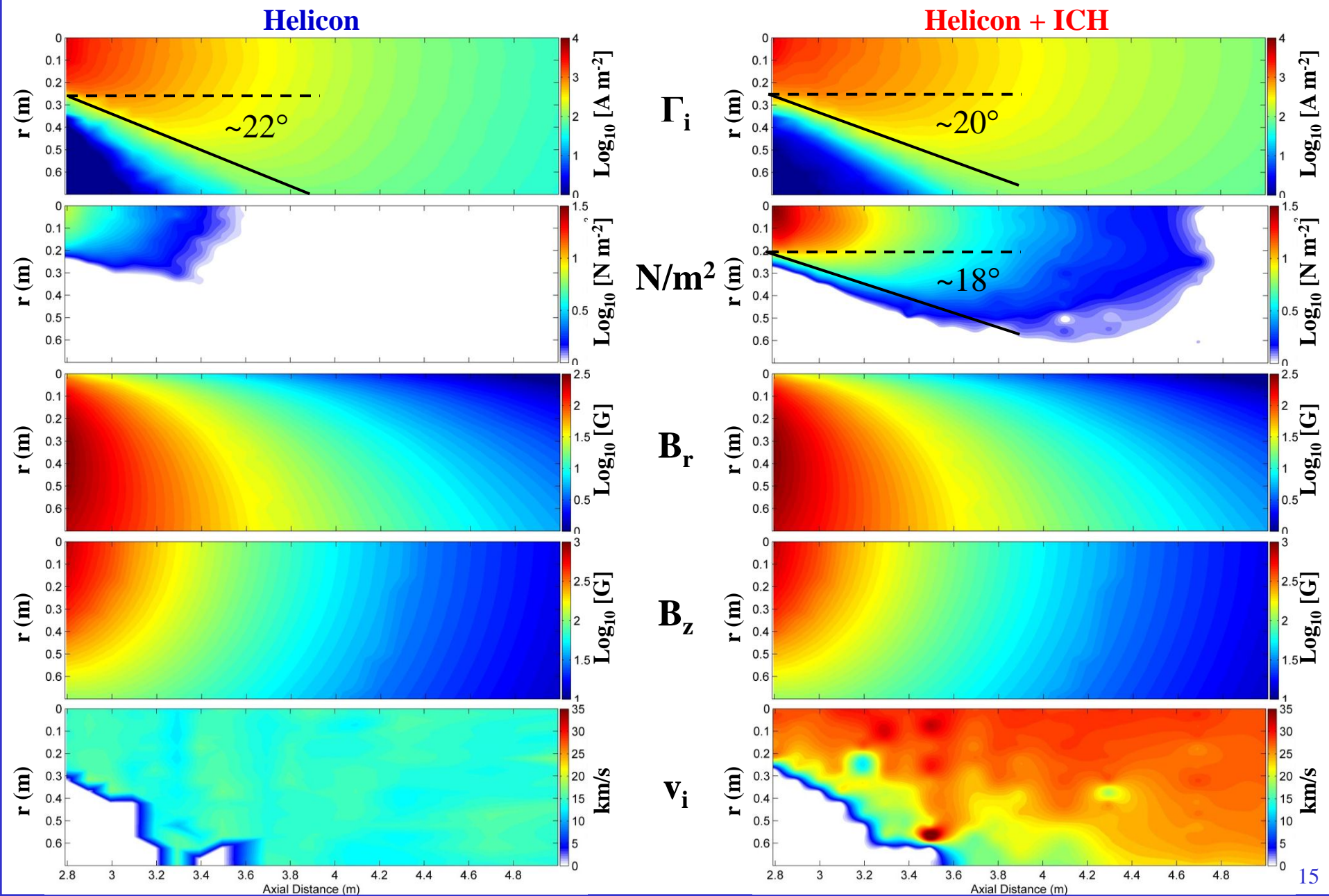


Photo Credit: AARC

- 2 m x 5 m ballscrew driven Translation Stage is used to reposition plume diagnostics
- Controlled using vacuum-rated Stepper motors capable of 0.1 mm position resolution
- All diagnostics are mounted upon a standard laser table interface and raised ~ 30 cm the surface
- Graphite and Grafoil™ shielding used to minimize sputtering
- High-Frequency electric field probe is recessed (with full line of sight) to minimize high heat loads.

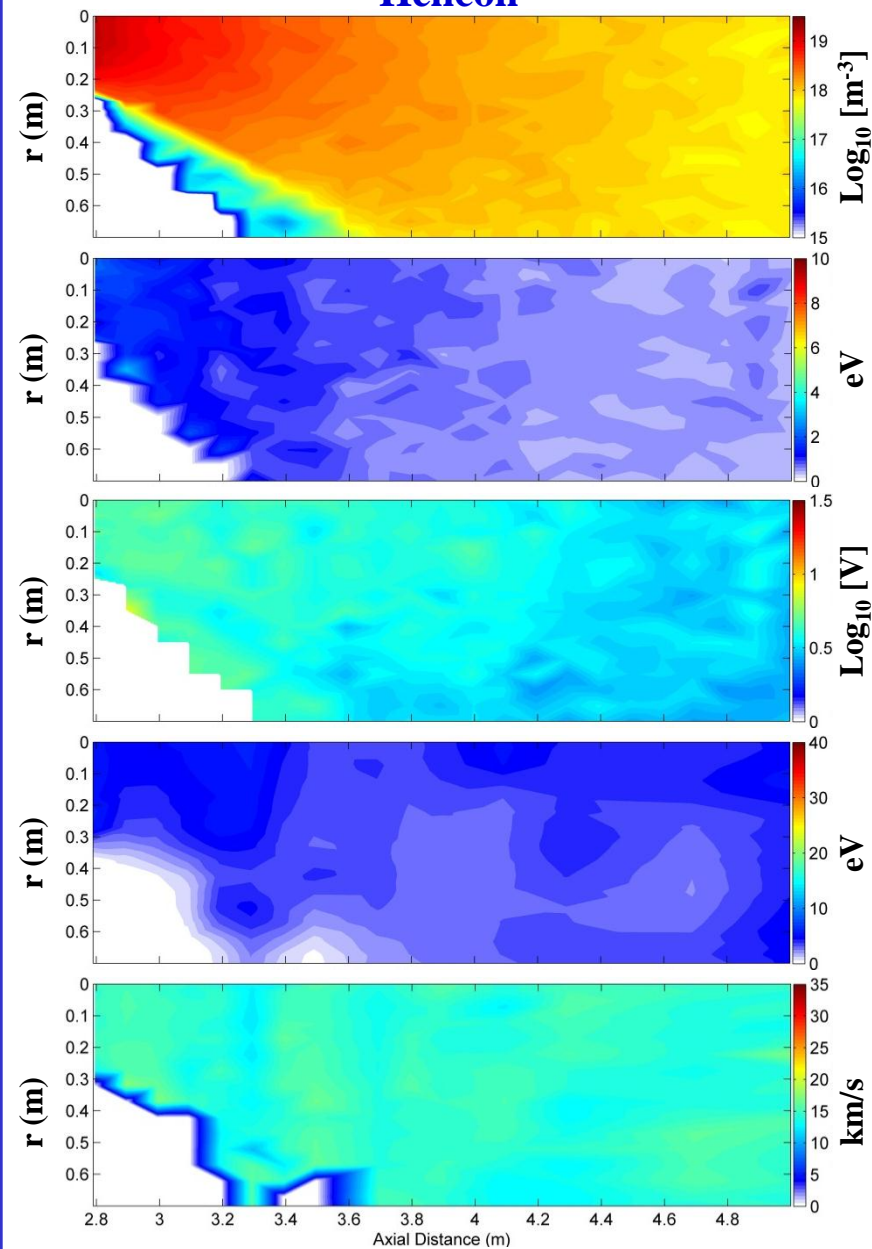
Diagnostic	X offset (mm)	Y offset (mm)	Z offset (mm)	Angle (Deg.)
Ion Flux Probe Array (Lower)	-257.2 - 0	177.8	-106.7	0
Ion Flux Probe Array (Upper)	0 - 270	254	-106.7	0
Plasma Momentum Flux Sensor (Primary)	0	-50.8	-106.7	0
Plasma Momentum Flux Sensor (Backup)	-85.7	-0.127	-106.7	0
Magnetometer	0	50.8	-106.7	0
Guard-Ring Probe	0	101.6	-106.7	0
Retarding Potential Analyzer	0	-177.8	-106.7	0 - 90
Electric Field Probe	0	-114.3	333.4	0

Measured Plasma Properties

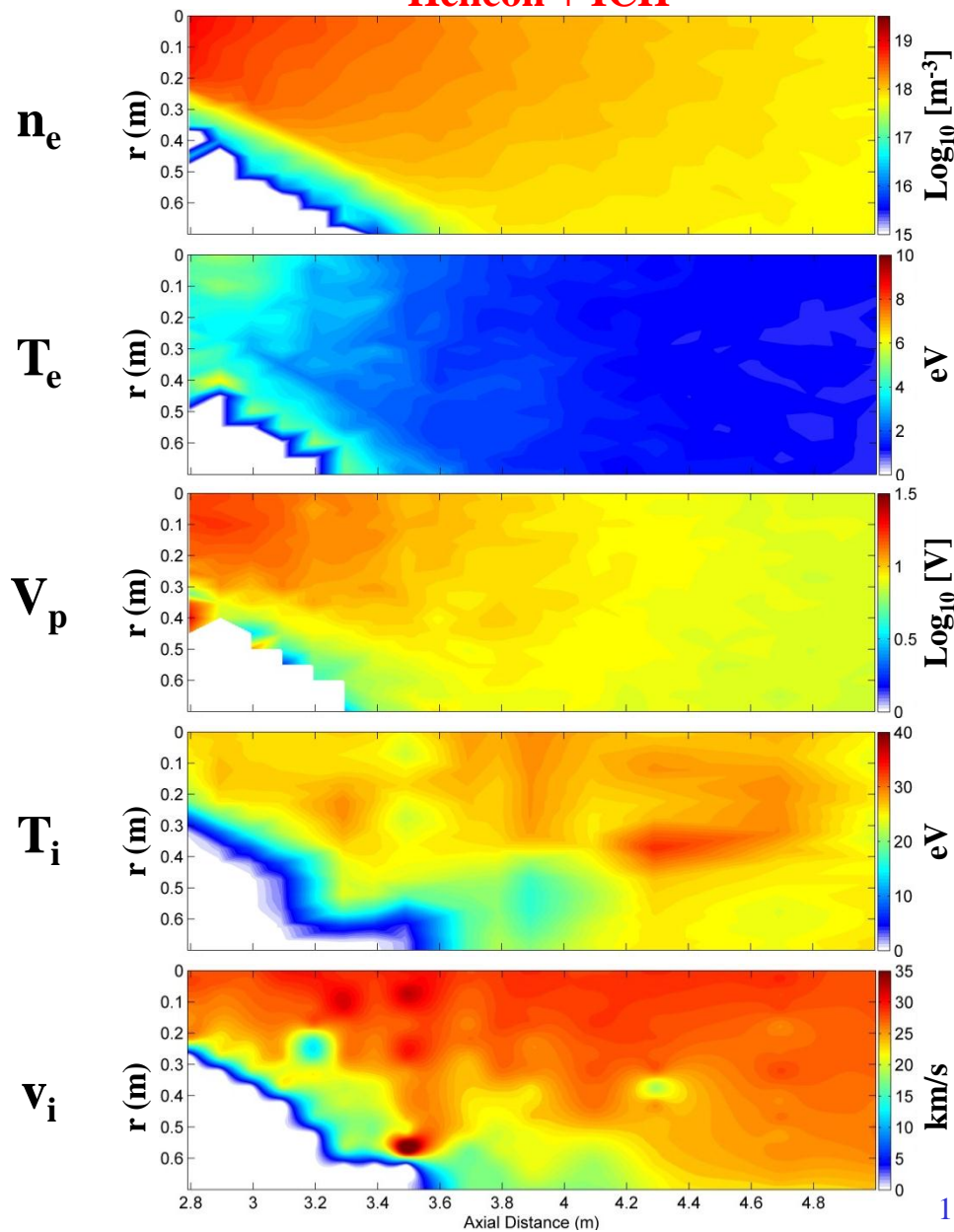


Measured Plasma Properties

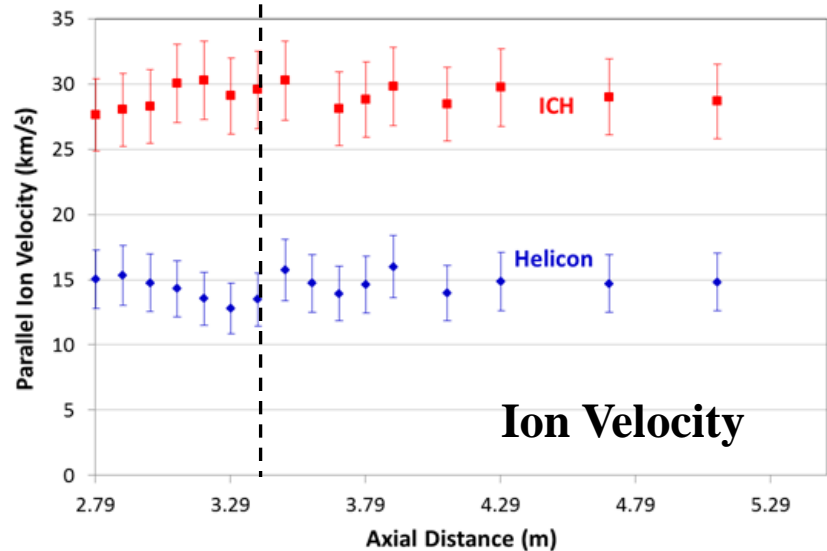
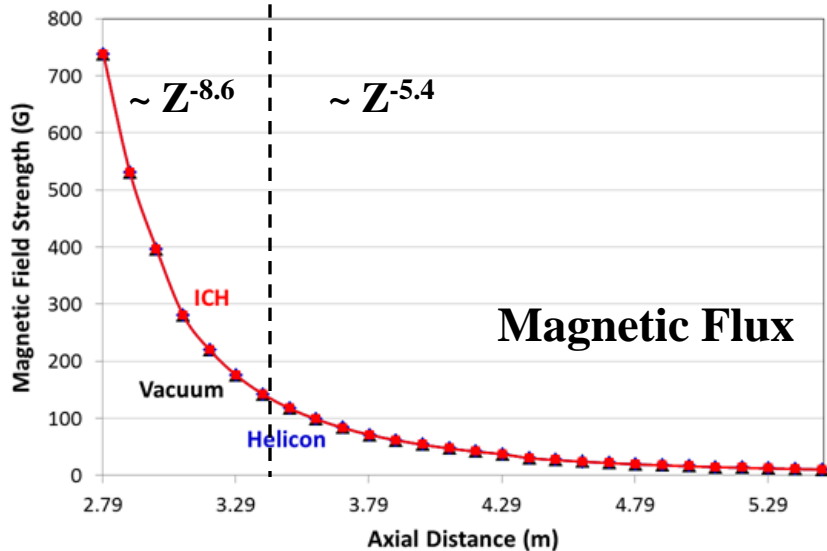
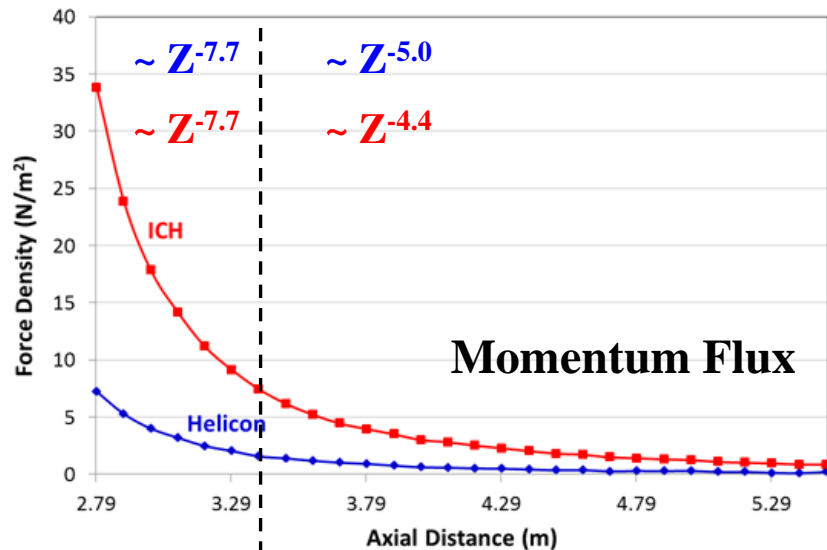
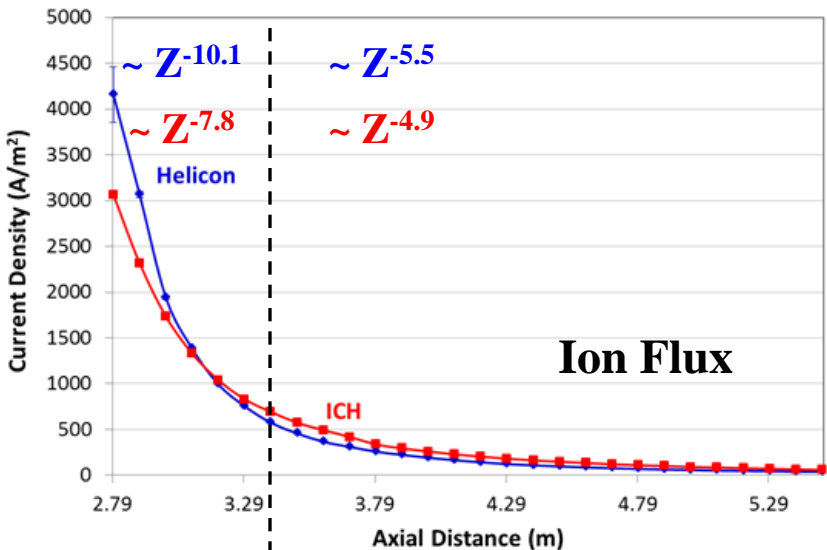
Helicon



Helicon + ICH

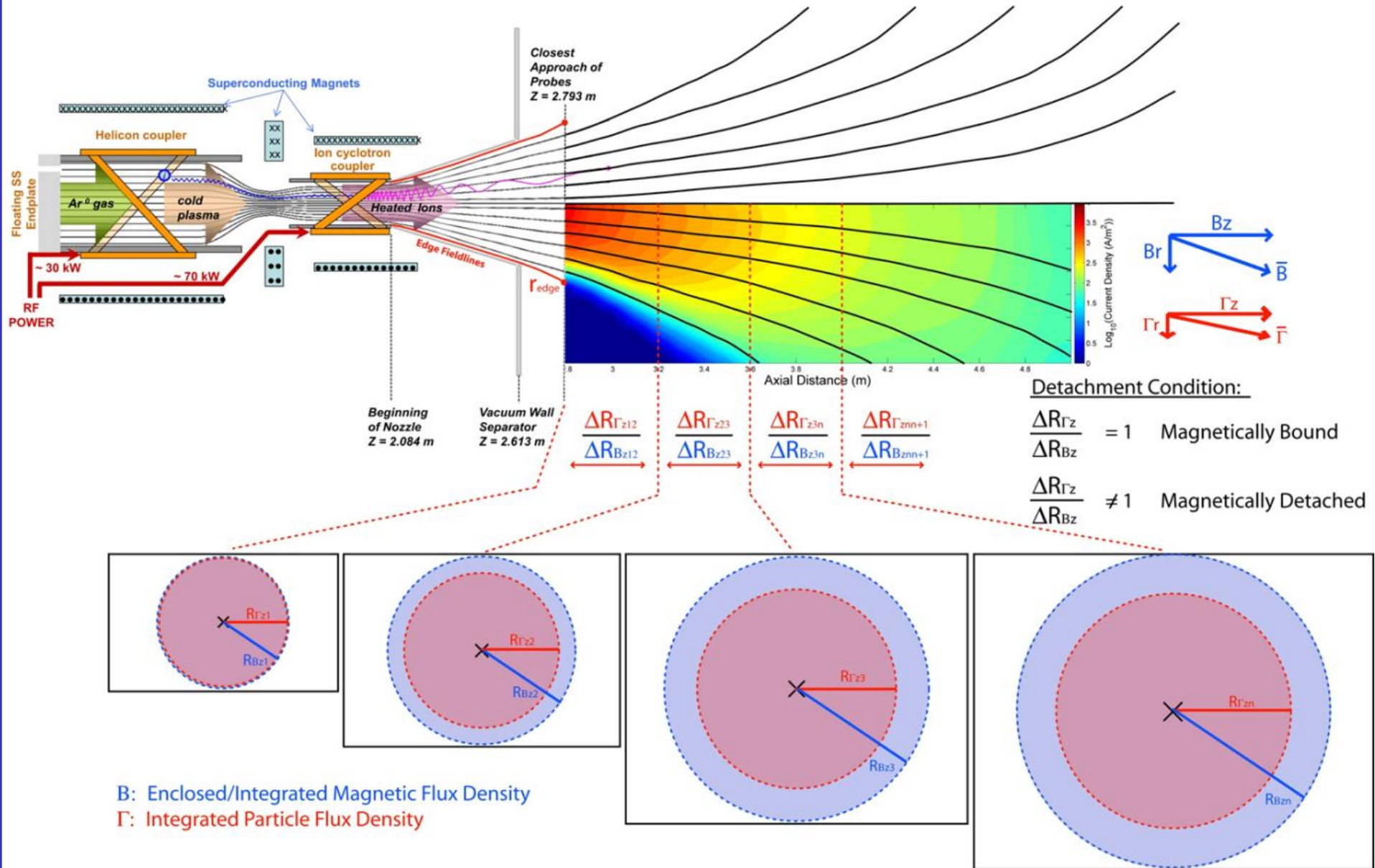


Axial Power Law Scaling



Coefficient of determination > 0.995 for each scaling

Method of Mapping Ion Expansion (Trajectories)



Compare mapped lines of constant ion flux to magnetic flux

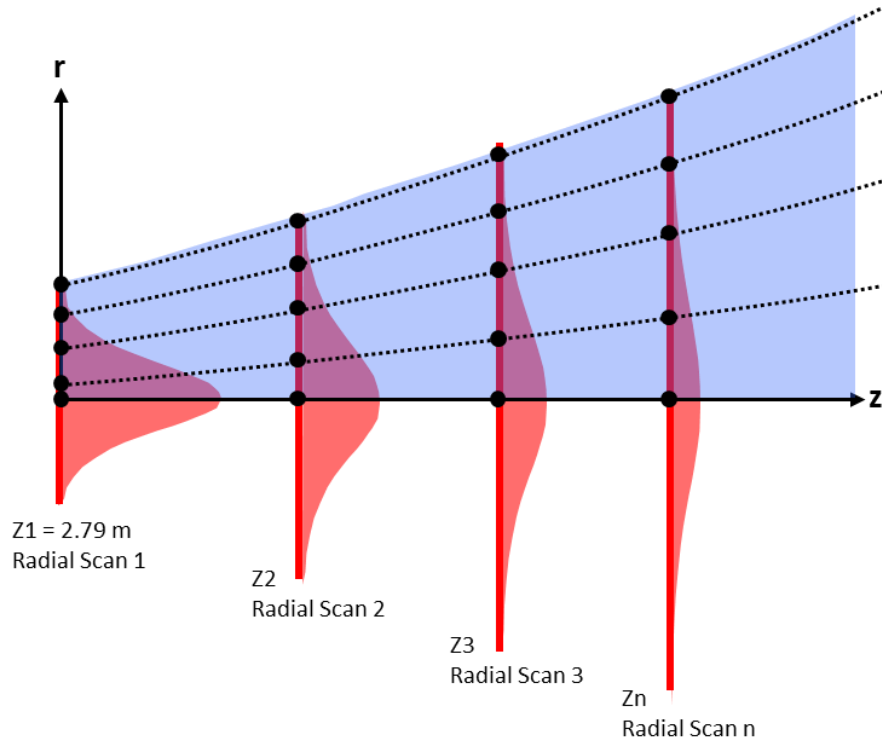
Continuity equation at steady state:

$$\frac{\partial \rho}{\partial t} + \nabla \cdot (\rho \bar{u}) = S - L \approx 0$$

- Mapped ion flux is numerically integrated radially
- Discrete values, f_i , of this ion flux are compared to the exit values and tracked according to (r, z) position
- Magnetic flux is treated similarly but integrated out to the ion flux initial position enclosing the magnetic flux.

Integrated Ion/Magnetic Flux: $\Gamma_{iz}(r) = 2\pi \int_0^r \frac{J_{iz}}{q} r dr$ $\Phi_z(r) = 2\pi \int_0^r B_z r dr$

Discreet plume fractions: (0.05 – 0.95) $f_i = \frac{\Gamma_{iz}(r)}{\Gamma_{iz1}(r_{edge})}$ $f_\Phi = \frac{\Phi_z(r)}{\Phi_{z1}(r_{fi})}$



It is useful to compare trends in the lines of constant integrated flux using parameters known as the Slope Ratio (SR):

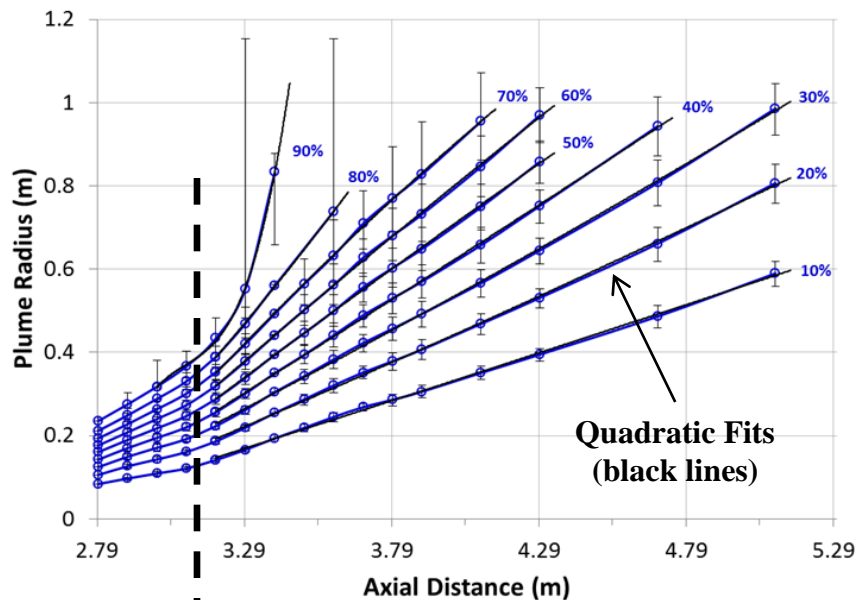
$$SR = \frac{m_{\Gamma_n}}{m_{B_n}} = \frac{\left(\frac{dR_{\Gamma_n}}{dz}\right)}{\left(\frac{dR_{B_n}}{dz}\right)} = \frac{R_{\Gamma_{n+1}} - R_{\Gamma_n}}{R_{B_{n+1}} - R_{B_n}}$$

and the separation angle between the ion and magnetic flux called the Detachment Angle (θ_n):

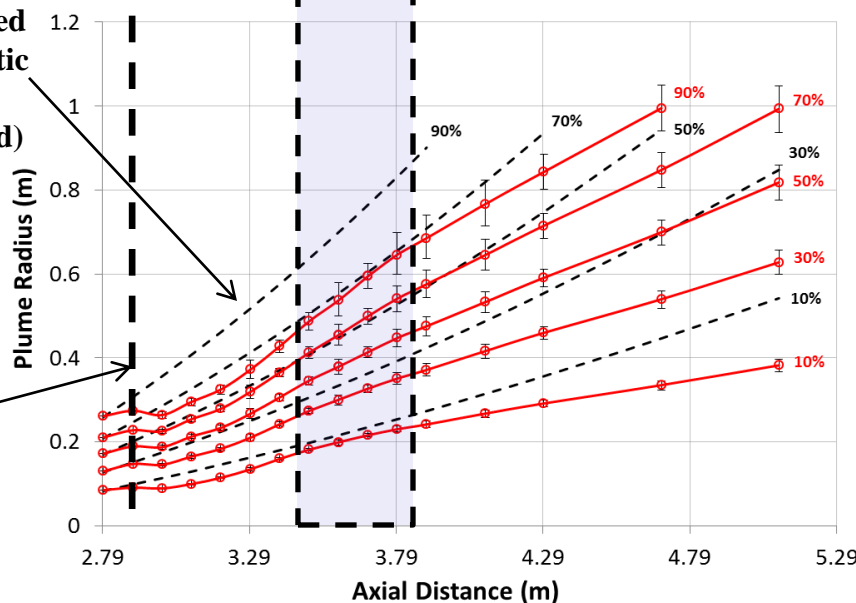
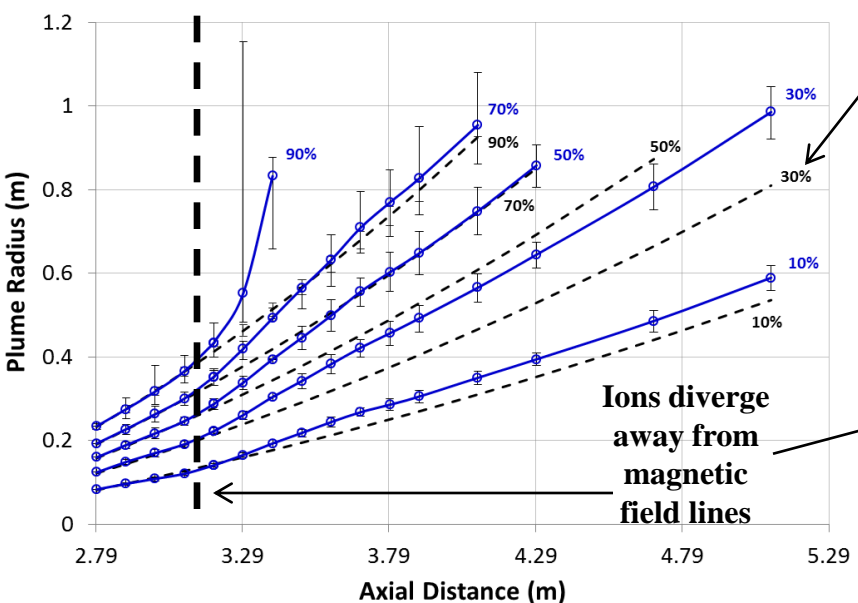
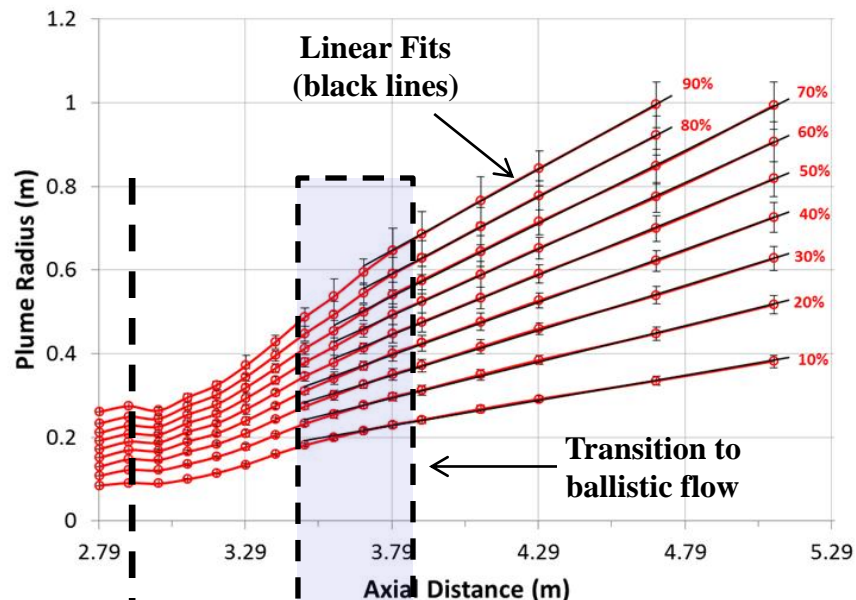
$$\theta_n = \tan^{-1} \left(\frac{m_{B_n} - m_{\Gamma_n}}{1 + m_{B_n} m_{\Gamma_n}} \right)$$

Integrated Ion Flux

Helicon

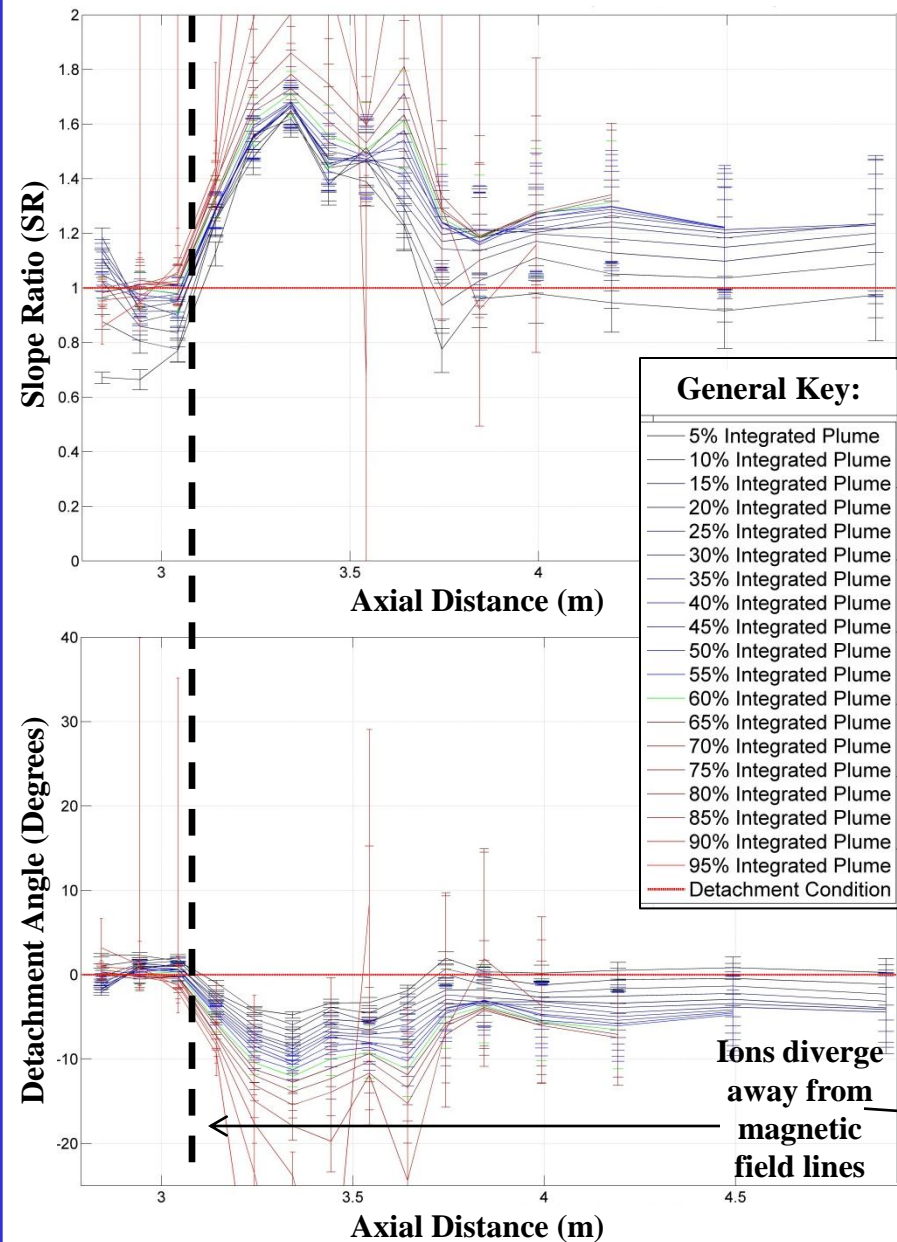


Helicon + ICH

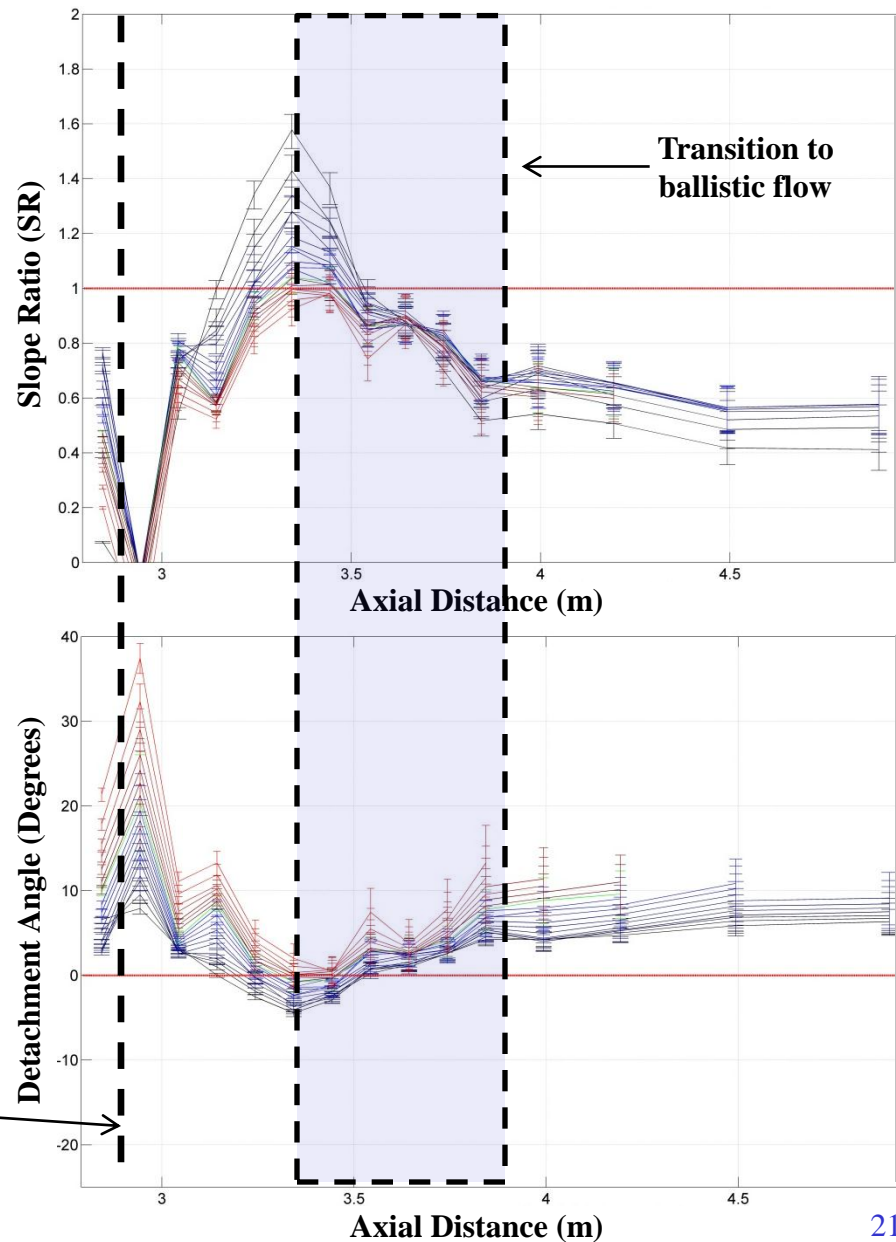


Ion flux slope ratio (SR) and Detachment Angle

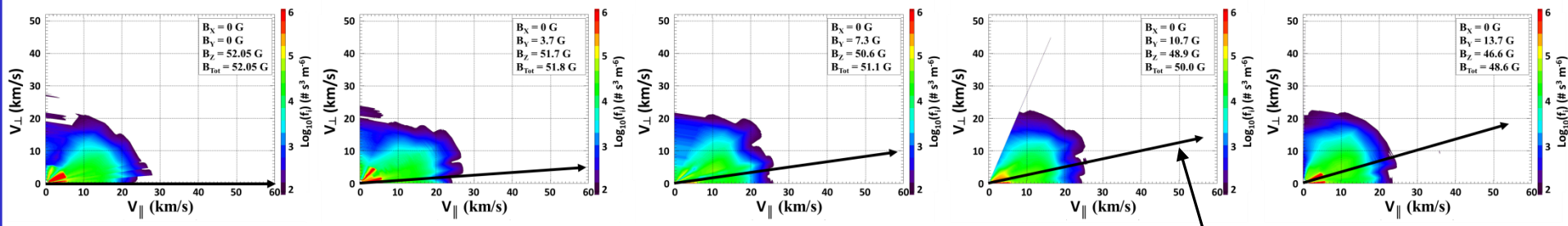
Helicon



Helicon + ICH



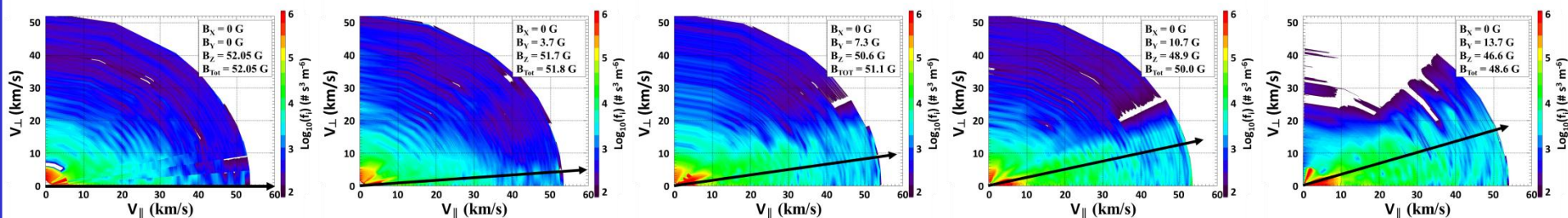
Detached Ions according to RPA Pitch Angles



↑ Helicon (30 kW) ↑

Local Magnetic Field Vector

↓ Helicon + ICH (100 kW) ↓



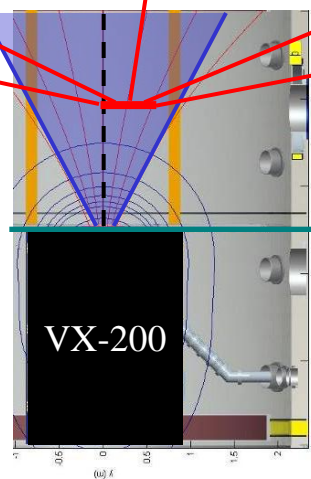
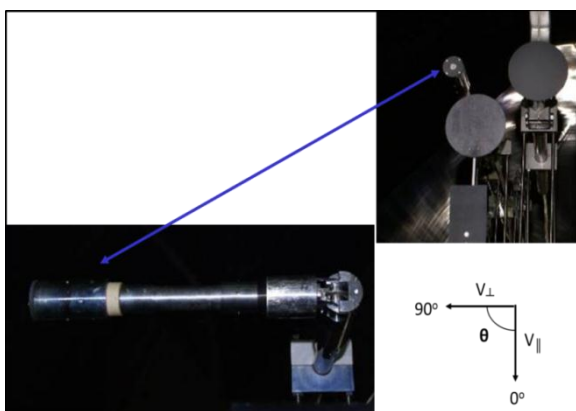
R = 0 m

R = 0.1 m

R = 0.2 m

R = 0.3 m

R = 0.4 m



- RPA was articulated from 0 - 90° along a radius ~ 2 m from the nozzle throat
- The local magnetic field does not seem to have an effect on the velocity distribution
- In the hot ion case the velocities remain directed along the nozzle axis.

Comparing theory with the data...

Let's start by looking at the collisional properties of the plume.

Collisional Diffusion: On axis data

Collision frequency for a test particle/field particle model:

$$v_{\alpha\beta}(V) = \frac{n_{\beta}q^4 \ln \Lambda}{2\pi\epsilon_0^2 m_{\alpha}^2 V^3} [\phi(a_{\beta}V) - \psi(a_{\beta}V)]$$

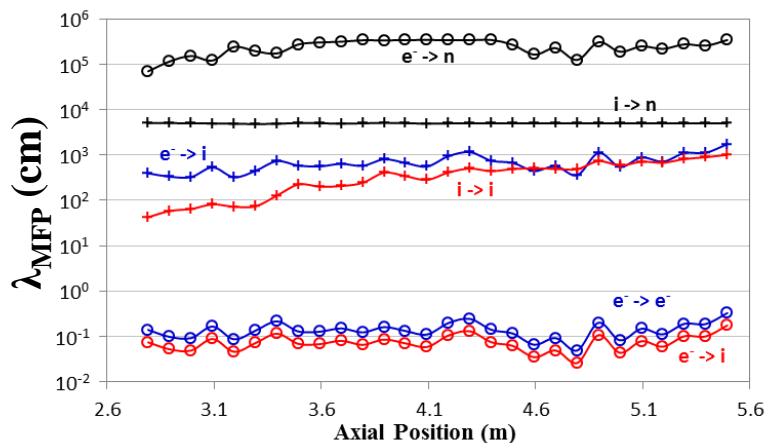
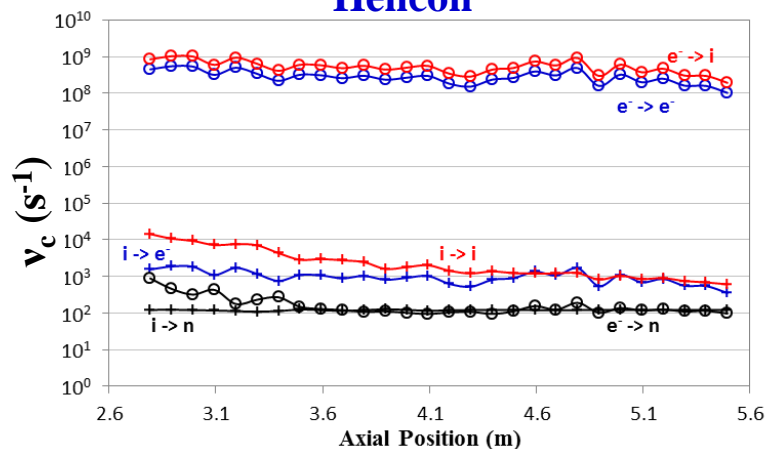
$$a_{\beta}^2 = \frac{m_{\beta}}{2k_B T_{\beta}}$$

Assume asymptotic values for the error function/derivatives:

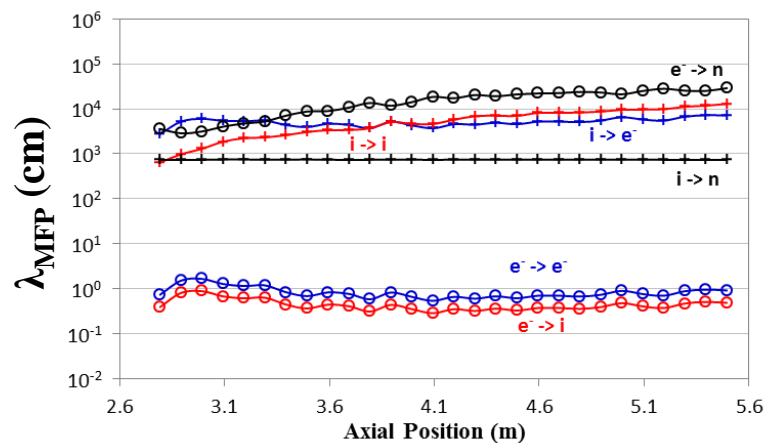
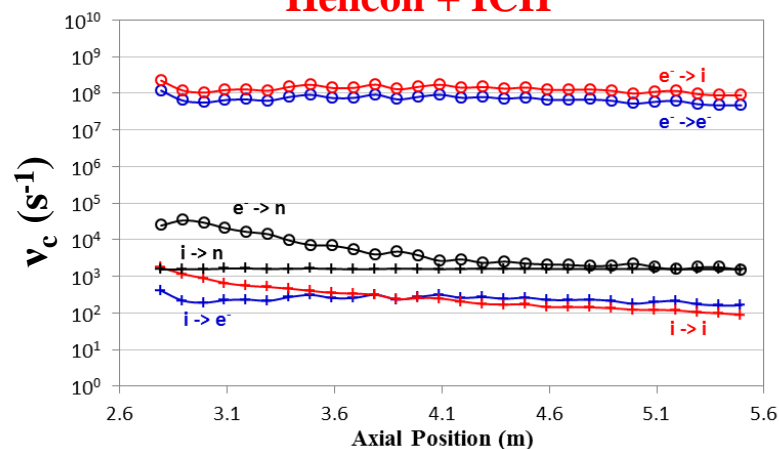
$$x \rightarrow 0: \phi(x) \sim 2x/\sqrt{\pi}, \psi(x) \sim 2x/3\sqrt{\pi}$$

$$x \rightarrow \infty: \phi(x) \sim 1, \psi(x) \sim 1/2x^2$$

Helicon



Helicon + ICH



Key:

Symbols
(Test Particle):

O → Electron
+ → Ion

Color
(Field Particles):

— Neutrals
— Electrons
— Ions

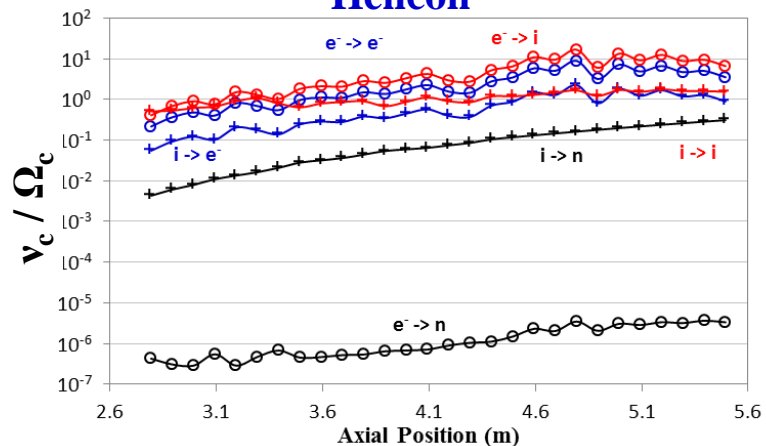
Ions are weakly collisional; electrons are collisional with short mean-free-paths.

Are these collisions, *electron*→*electron* and *electron*→*ion*, strongly coupled to the plasma?

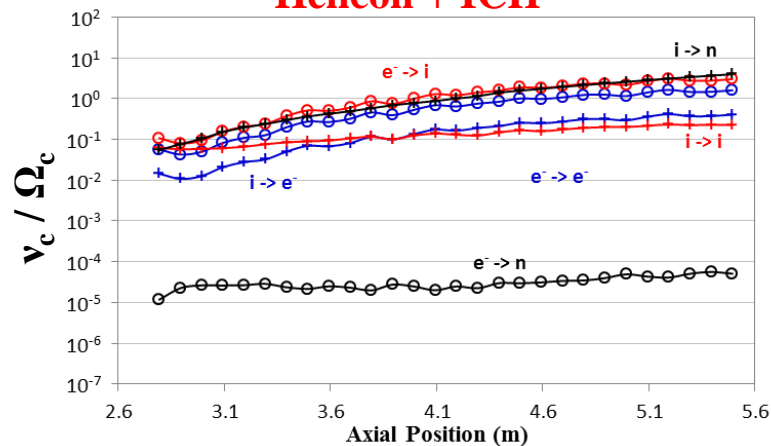
Collisional Diffusion: On axis data

The electrons initially complete several gyrations prior to a collision, but downstream begin to collide at least once per gyration as the Larmor radius grows. These values are reduced at higher ion energy.

Helicon



Helicon + ICH



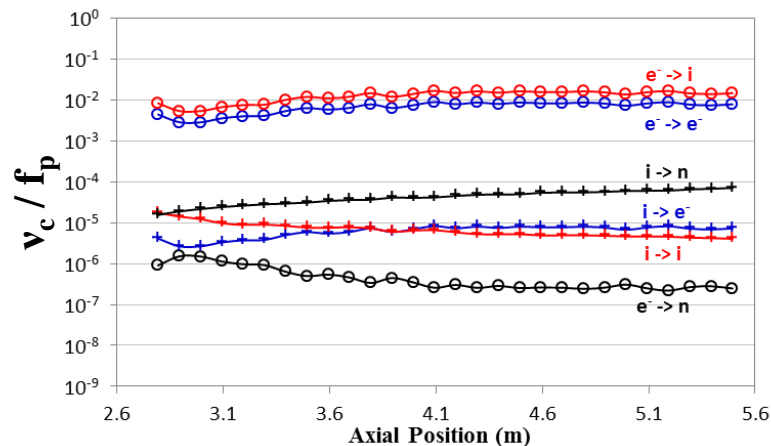
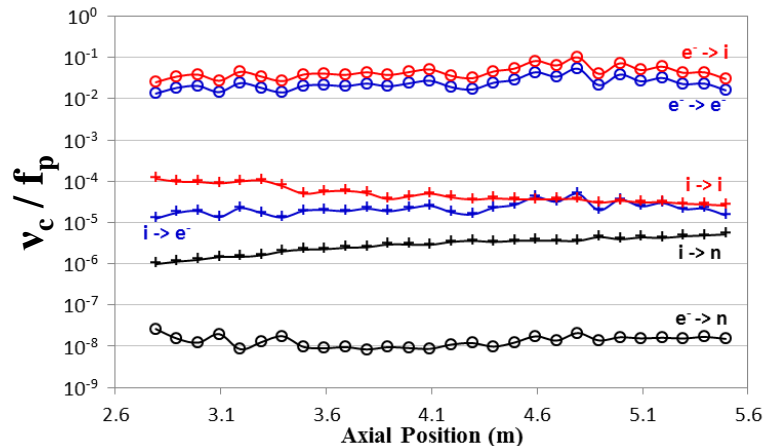
Key:

Symbols (Test Particle):

O → Electron
+ → Ion

Color (Field Particles):

— Neutrals
— Electrons
— Ions



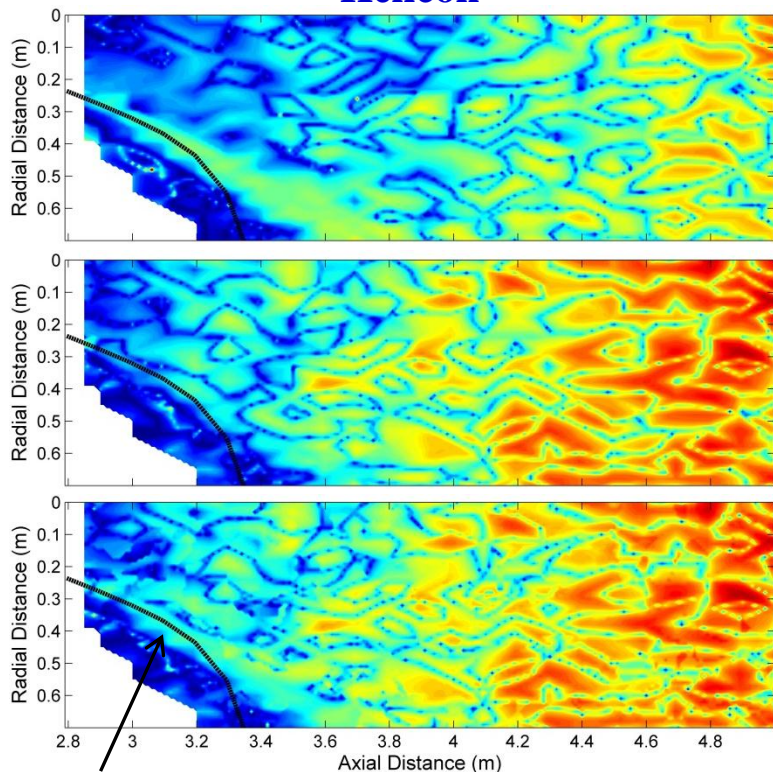
All of the particle collisions appear weakly coupled ($v_c / f_p \ll 1$) and do not seem to affect the plasma frequency for these ion energy levels.

Where is electron collisional transport occurring and can it account for detachment?

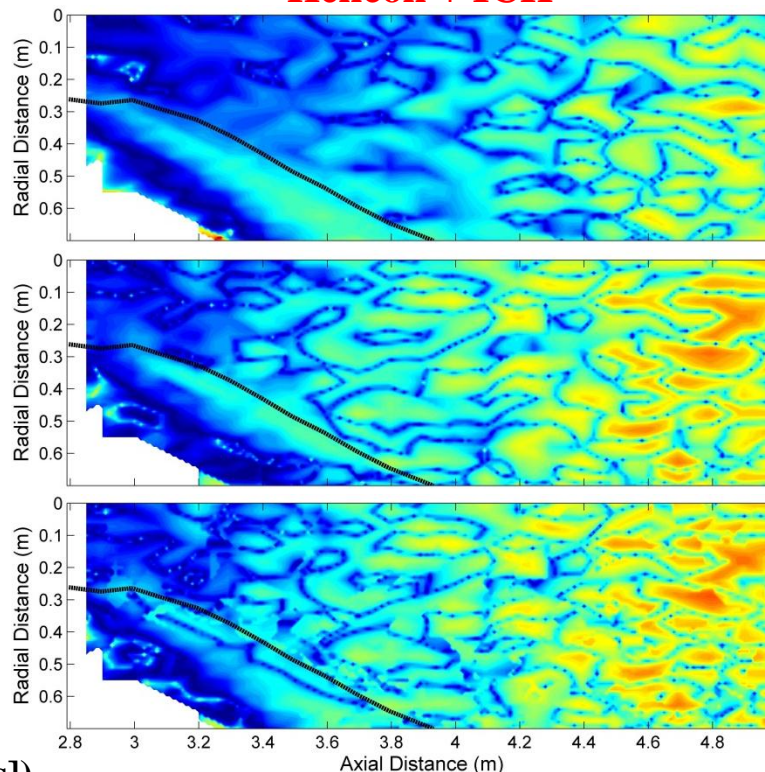
Electron → Electron Collision Cross-Field Velocity

Occurring too slow and would not result in net transport anyways.

Helicon



Helicon + ICH



Diffusion

Mobility

Net

Effective
Plume Edge
(90% Ion Flux)

$$U_{\perp} = \underbrace{\mu_{ee} E}_{\text{Mobility Component}} - \underbrace{D_{ee} \frac{\nabla n}{n}}_{\text{Diffusion Component}} + \frac{u_{E \times B} + u_D}{1 + \left(\frac{v_{ee}}{\Omega_e}\right)^2}$$

Azimuthal

Net Electron
Cross Field
Velocity

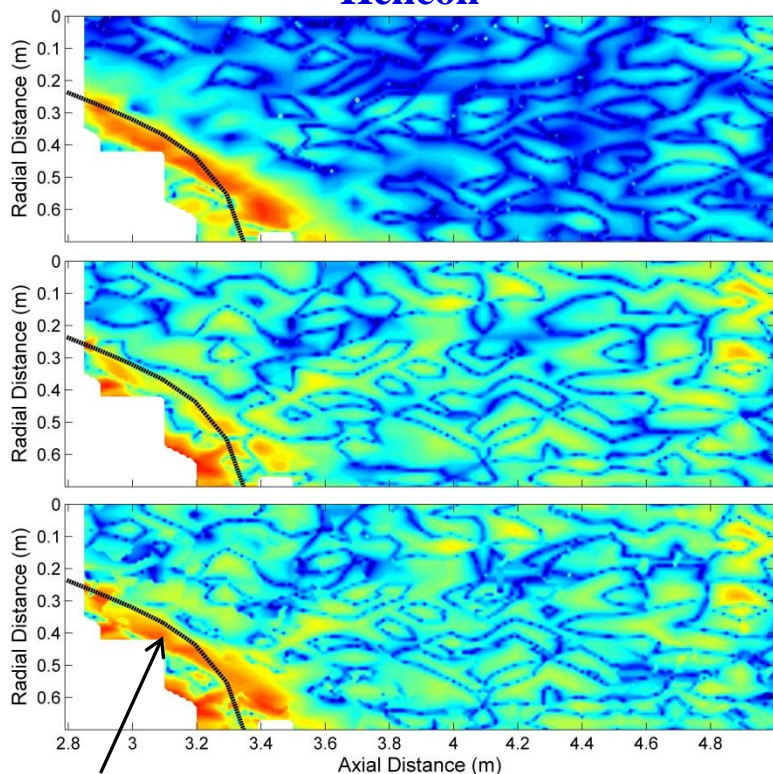
$$D_{ee} = \frac{v_{te}^2}{v_{ee}} \frac{1}{1 + \left(\frac{\Omega_e}{v_{ee}}\right)^2}$$

$$\mu_{ee} = \frac{D_{ee}}{T_e}$$

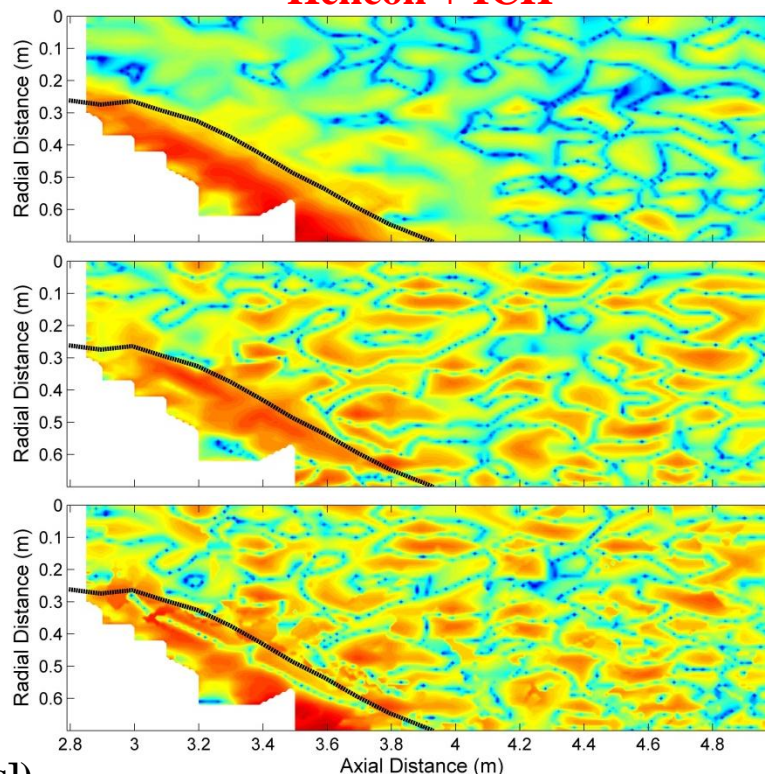
Electron → Ion Collision Cross Field Velocity

Collisional diffusion alone is insufficient to account for detachment and maintain pace with departing ions. Cross-field velocities are ~ 10x too slow. Additional processes are required.

Helicon



Helicon + ICH



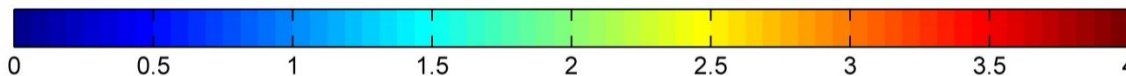
Diffusion

Mobility

Net

$\text{Log}_{10}(U_{\perp} \text{ [m/s]})$

Effective
Plume Edge
(90% Ion Flux)



Net Electron Cross Field Velocity

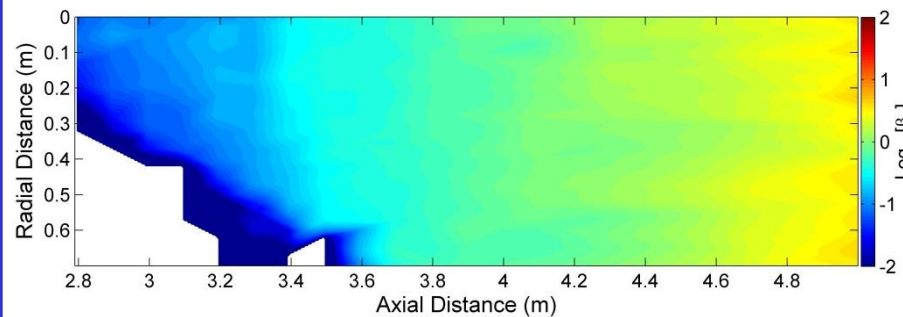
$$U_{\perp} = \underbrace{\mu_{ei} E}_{\text{Mobility Component}} - \underbrace{D_{ei} \frac{\nabla n}{n}}_{\text{Diffusion Component}} + \underbrace{\frac{u_{E \times B} + u_D}{1 + \left(\frac{v_{ei}}{\Omega_e}\right)^2}}_{\text{Azimuthal}}$$

$$D_{ei} = \frac{v_{te}^2}{v_{ei}} \frac{1}{1 + \left(\frac{\Omega_e}{v_{ei}}\right)^2}$$

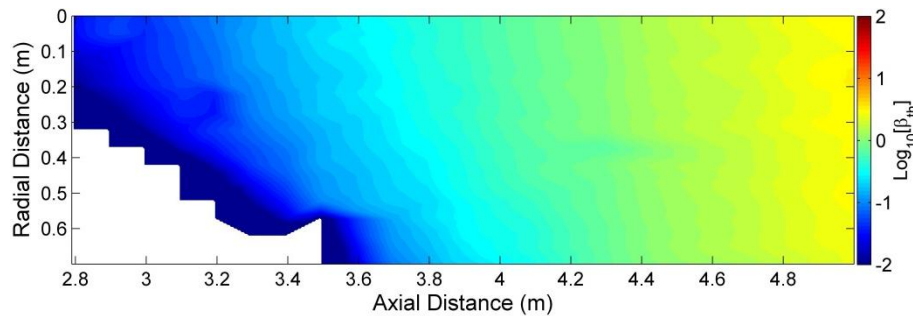
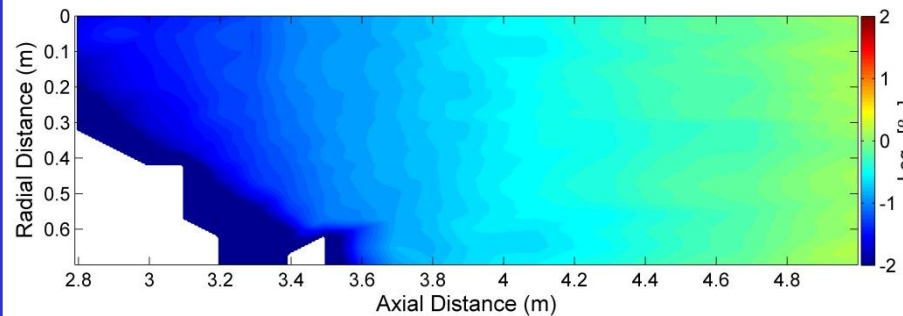
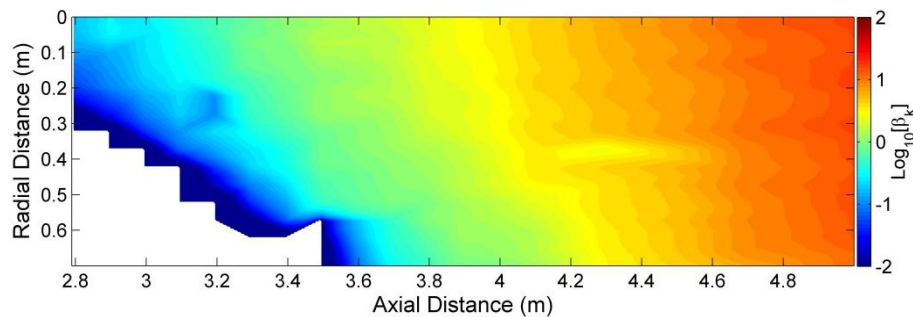
$$\mu_{ei} = \frac{D_{ei}}{T_e}$$

MHD Field Line Stretching

Helicon

 β_k


Helicon + ICH

 β_{th}


Kinetic Beta:
$$\beta_k = \frac{n_i m_i v_i^2}{(B^2 / \mu_0)}$$

Thermal Beta:
$$\beta_{th} = \frac{n k_B T_i}{(B^2 / 2\mu_0)}$$

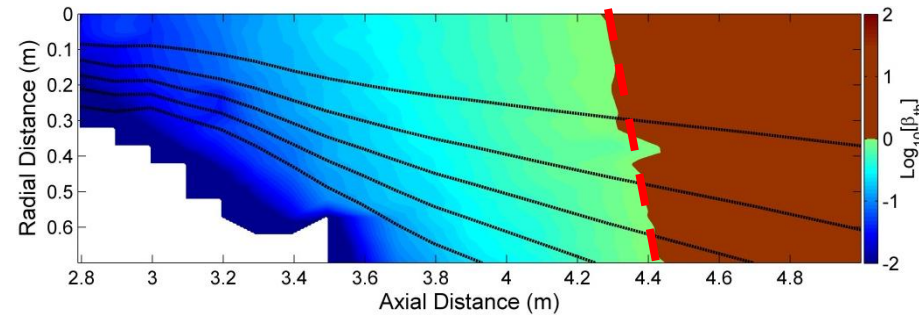
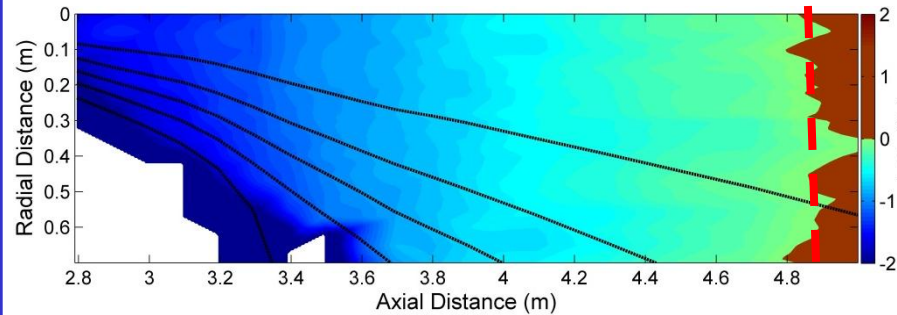
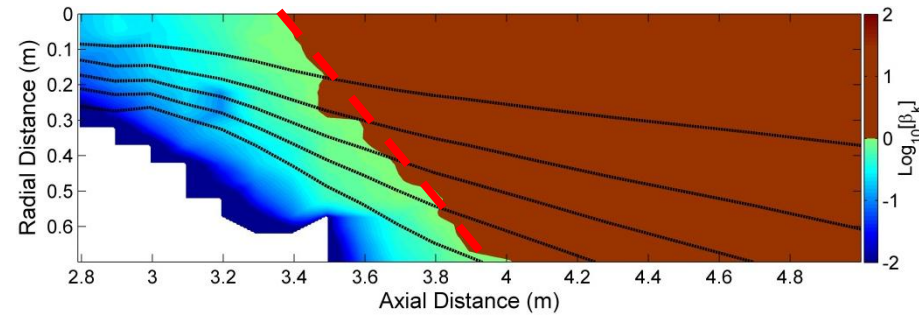
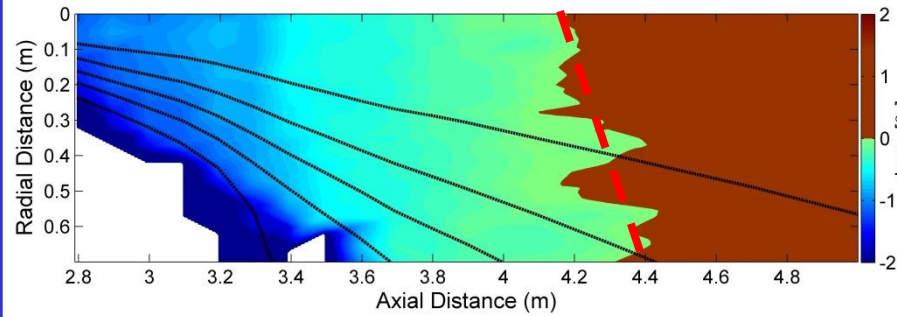
MHD Field Line Stretching

Helicon

β_k

Helicon + ICH

β_{th}



Kinetic Beta:
$$\beta_k = \frac{n_i m_i v_i^2}{(B^2 / \mu_0)}$$

Thermal Beta:
$$\beta_{th} = \frac{nk_B T_i}{(B^2 / 2\mu_0)}$$

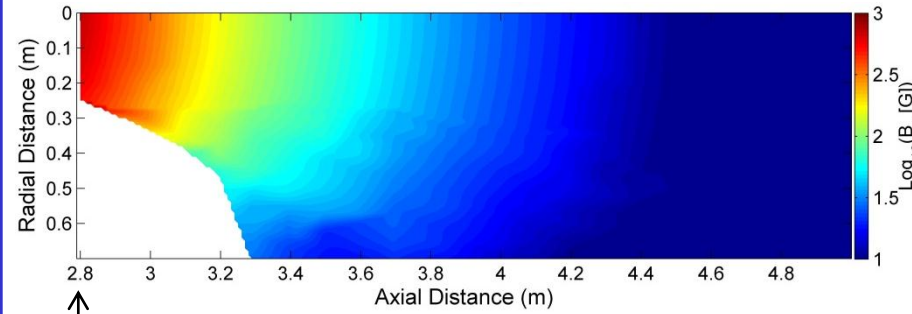
- Both kinetic and thermal beta exceed unity in the plume during all phases of operation.
- This demarcation shifts upstream with increasing ion energy.
- The super-Alfvénic transition interestingly coincides with ion expansion linearization during ICH.
- The plume between $\beta_{th} < 1 < \beta_k$ should be energetically capable to stretching the field lines out to infinity.
- Is this effect observed?

Simulated MHD plasma magnetic field

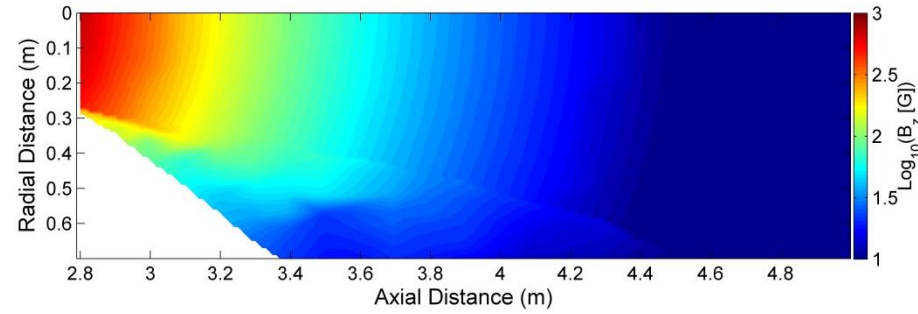
Helicon

Simulation

Helicon + ICH



B_z



z_0

$$B_z(r, z) = B_0 \frac{z_0^2}{z^2} \begin{cases} 1, & r \leq r_{rw} \\ \frac{1}{9} [M_A(z \tan \theta_0 - r) + 2(z - z_0)]^2 (z - z_0)^{-2}, & r_{rw} < r < r_{pv} \\ 0, & r_{pv} \leq r \end{cases}$$

Rarefaction Wave location: $r_{rw} = z \tan \theta_0 \left[1 - \frac{1}{M_A \tan \theta_0} \left(1 - \frac{z_0}{z} \right) \right]$

Plasma-Vacuum interface: $r_{pv} = z \tan \theta_0 \left[1 + \frac{2}{M_A \tan \theta_0} \left(1 - \frac{z_0}{z} \right) \right]$

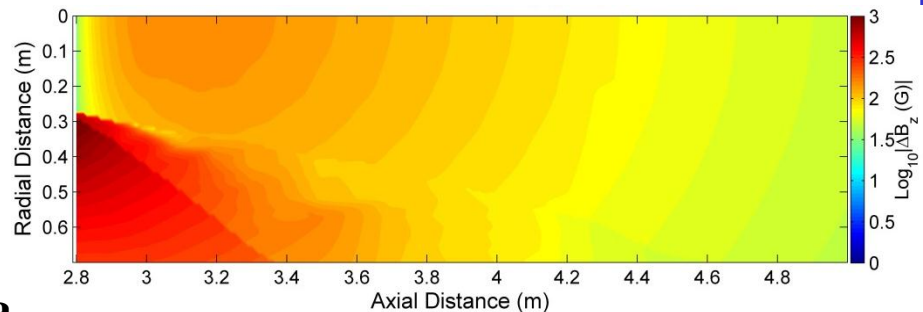
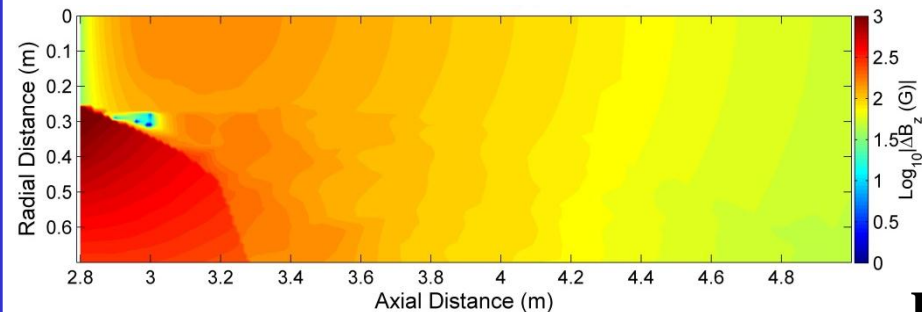
- Simulated magnetic field during plasma operation using Breizman (2008) model that modifies Arefiev (2005) cold ion model to include hot ions (e.g. ICH).
- Assumes 22° & 20° nozzle divergence angles taken from mapped data for Helicon and ICH respectively.
- White regions mark locations for *zero magnetic field*

Simulated MHD plasma magnetic field

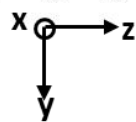
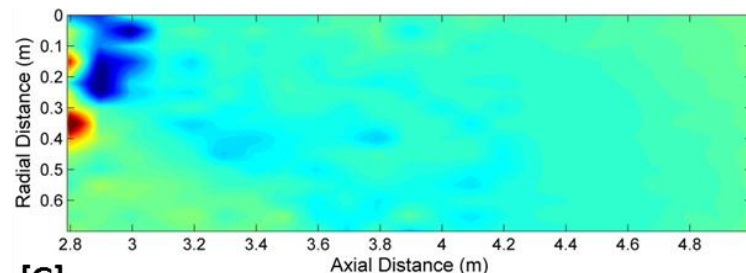
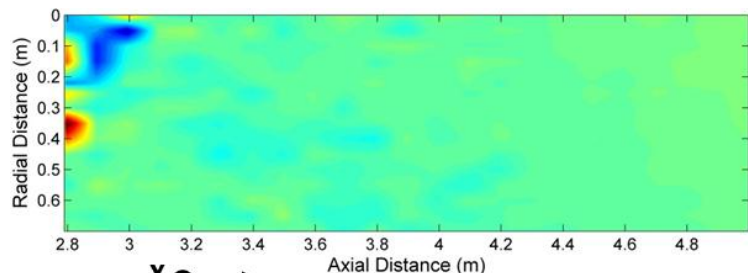
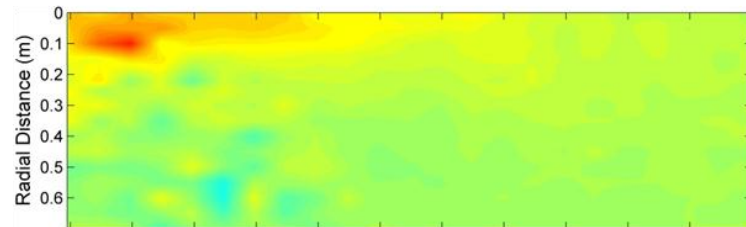
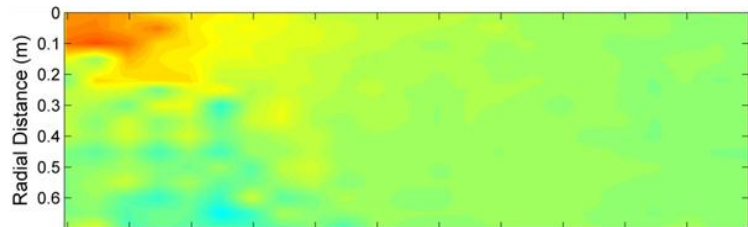
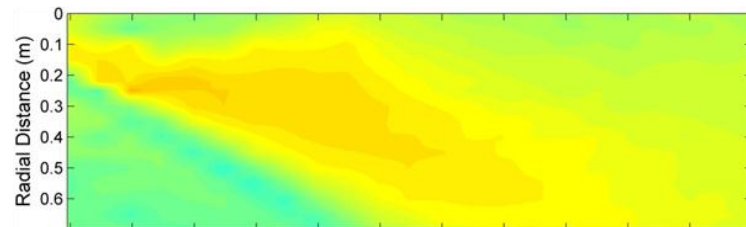
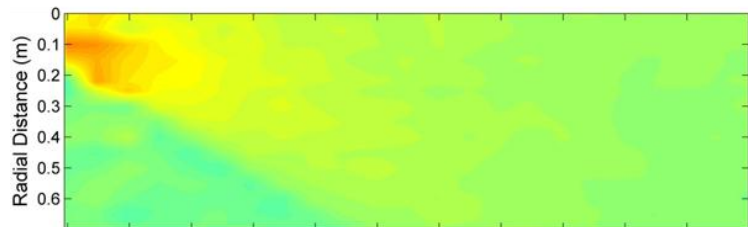
Helicon

Simulation

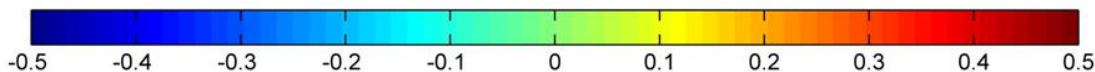
Helicon + ICH



Data



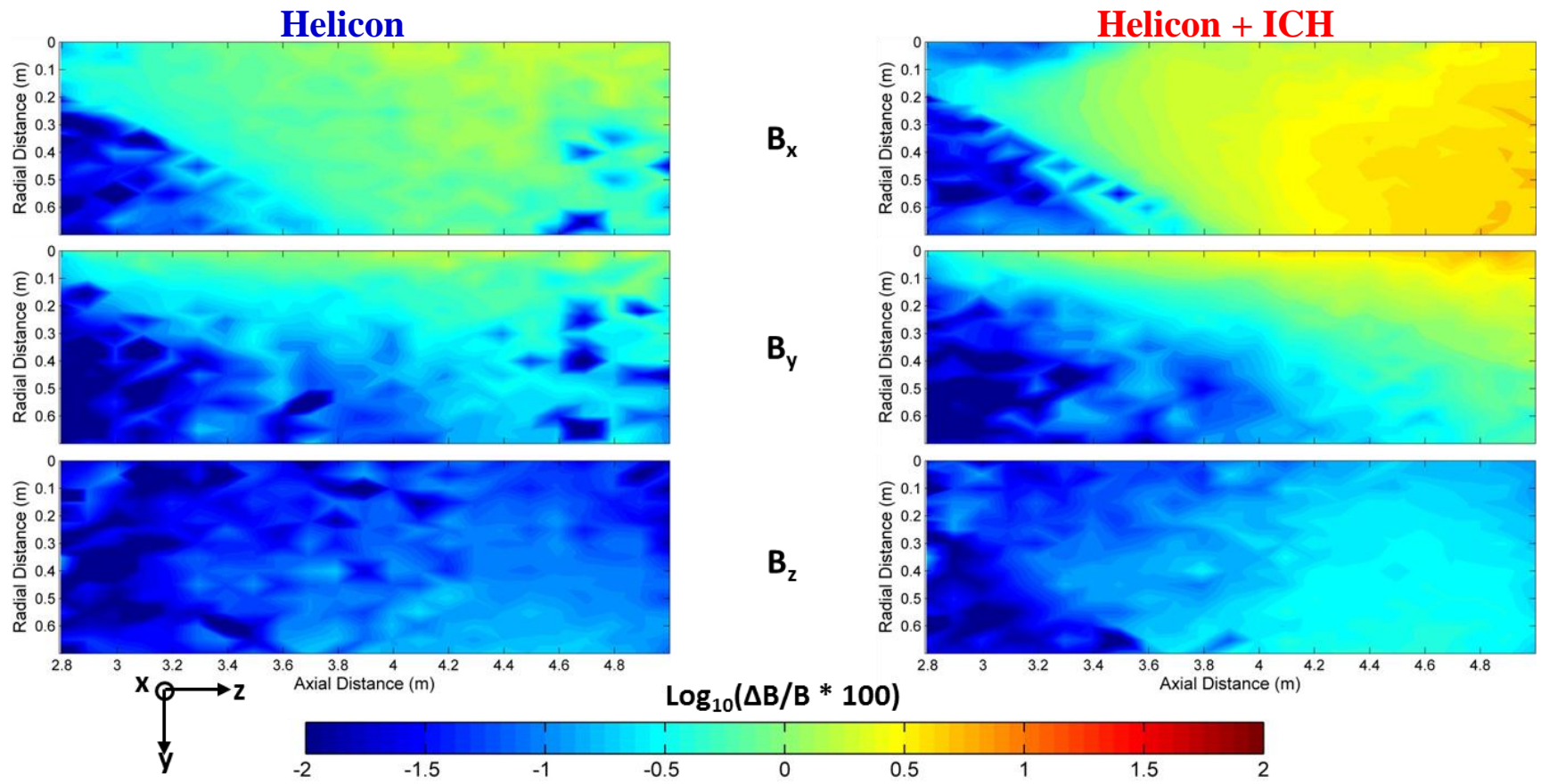
$B_{\text{plasma}} - B_{\text{vacuum}} \text{ [G]}$



Change in magnetic field from the applied vacuum field

Field line stretching does not appear to be occurring

- The magnitudes of the change in magnetic field are much less, by a few orders of magnitude, than the simulations predict despite the flow exceeding the Alfvén velocity.
- The change in magnetic field due to flowing plasma never exceeds 0.6 G (B_z) during Helicon and 0.78 G (B_z) during ICH.
- The largest changes as a % of local magnetic field occur at low field strengths and are at most $\sim 10\%$.
- **The data are inconsistent with the MHD field line stretching models.**



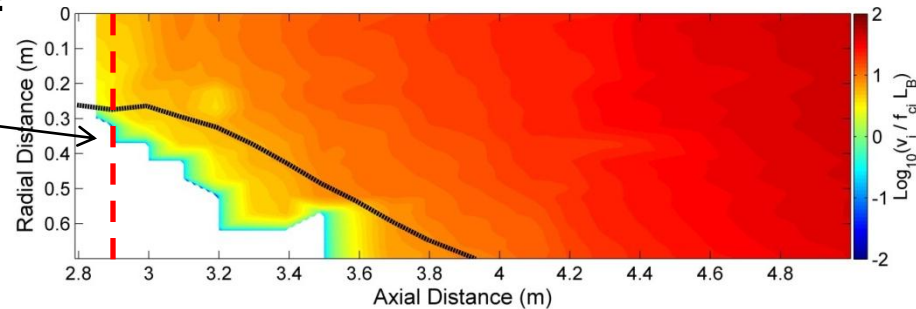
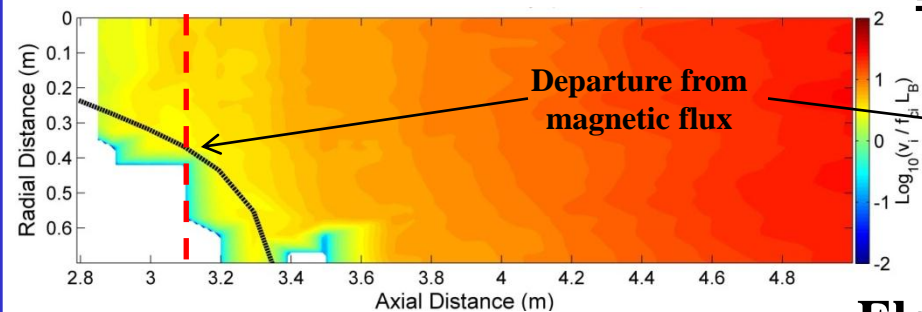
% change in magnetic field from the local field

Loss of Adiabaticity/Demagnetization

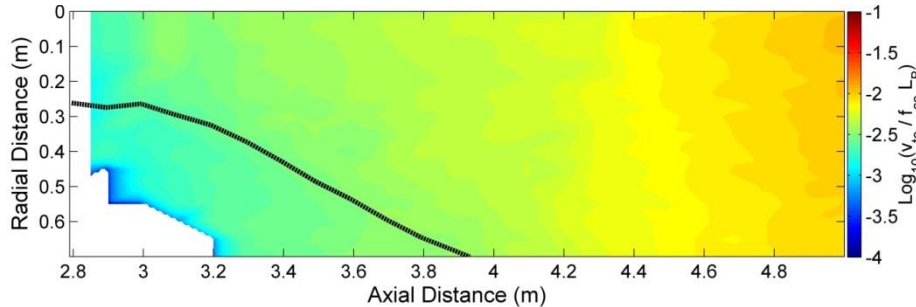
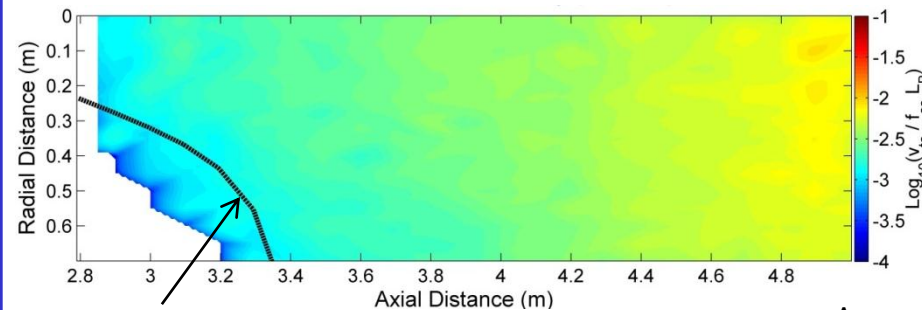
Helicon

Ion

Helicon + ICH



Electron



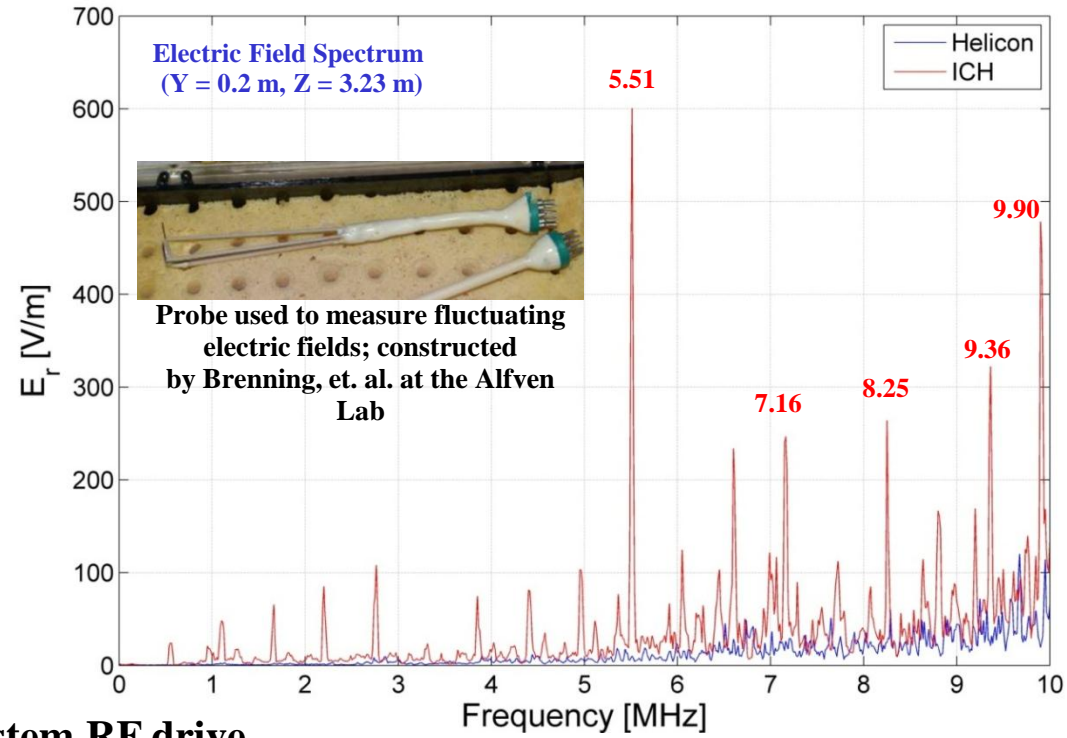
Effective Plume Edge
(90% Ion Flux)

$$\frac{\Delta r_c}{r_c} \approx \frac{\Delta \Omega_c}{\Omega_c} = \frac{v}{f_c L_B}$$

- Composite maps of the ion adiabaticity parameter show that this value exceeds unity for the majority of the measurable plume for both stages of operation.
- The magnetic moment is conserved until $2.9 \text{ m} < z < 3.1 \text{ m}$ during Helicon and $z < 2.9 \text{ m}$ during ICH where the values measure between $1.6 - 4.3$ and $2.2 - 4.9$ respectively.
- These axial regions overlap with the departure locations of the ion flux from the magnetic field.
- The electron adiabaticity parameter **never exceeds 0.013** over this measurement range, but demagnetization may be possible further downstream in the weaker magnetic field region.
- **Loss of adiabaticity is the likely ion detachment mechanism and presumably also mediates electron detachment further downstream.**

Plasma Turbulence

- It was seen earlier that electron cross-field velocities according to coulomb collisions are insufficient to keep up with the ions and prevent charge build-up
- Enhanced collision rates due to anomalous resistivity that may allow electrons to keep pace with the ions
- Anomalous resistivity may be driven by turbulence brought about by plasma instabilities
- A force balance between competing effects will govern net particle transport.
- Turbulence is observed as frequency dependent fluctuating electric fields (sample spectra →)
- The main peaks are not at either of the system RF drive frequencies.
- These peaks are within an order of magnitude of the lower hybrid frequency.
- *These spectra may be then graphed as a function of Position to see if any trends or structure align with previous data...*



Enhanced cross field mobility:

$$\mu_{\perp} = \frac{1}{B} \left[\frac{\Omega_e \tau_{eff}}{1 + \Omega_e^2 \tau_{eff}^2} \right]$$

Electric fields affecting transport:

$$\langle \tilde{E}_{\perp} \rangle_{AN} = \frac{v_{e\perp}}{\mu_{\perp}} = v_i \sin \theta B \left[\frac{1 + \Omega_e^2 \tau_{eff}^2}{\Omega_e \tau_{eff}} \right]$$

Anomalous transport

Ion trapping

$$\langle \tilde{E}_{\perp} \rangle_{IT} = \frac{m_i v_i^2}{q R_c}$$

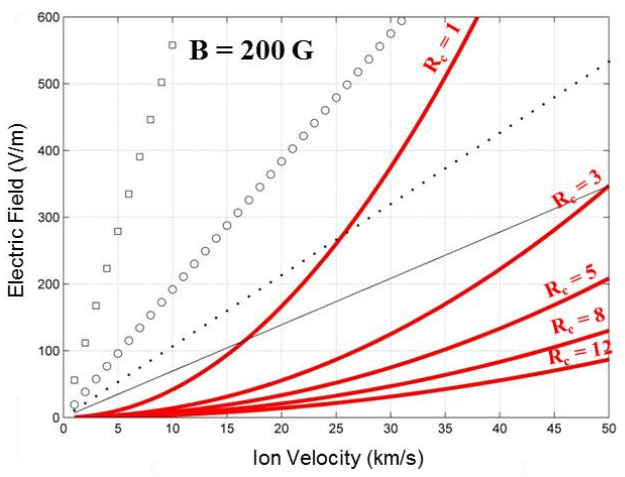
Effective Resistivity:

$$\eta_{eff} = \eta_c + \eta_{AN} \approx \eta_c + \frac{\langle \tilde{n}_e \tilde{E} \rangle}{q v_{de} \langle \tilde{n}_e \rangle^2}$$

Effective Momentum Transfer Time:

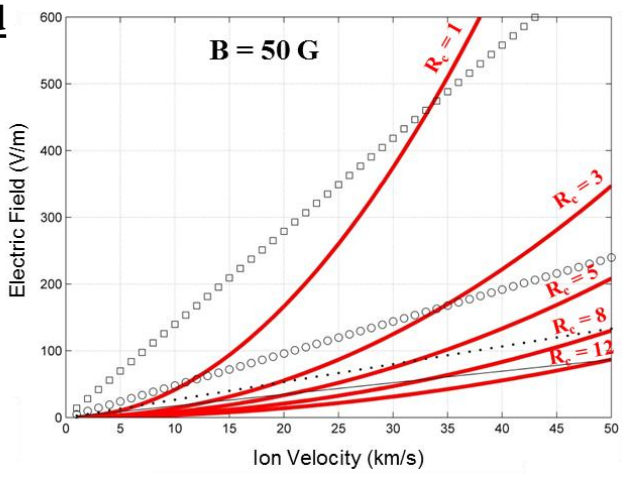
$$\tau_{eff} = \frac{m_e}{\eta_{eff} q^2 n_e}$$

Force Balance: Lowest Required Fields Dominate



Calculated

- Legend**
- : $\Omega\tau = 16$
 - : $\Omega\tau = 5.3$
 - : $\Omega\tau = 2.7$
 - : $\Omega\tau = 1$
 - (red) : Ion Trapping
- $\theta = 10^\circ$



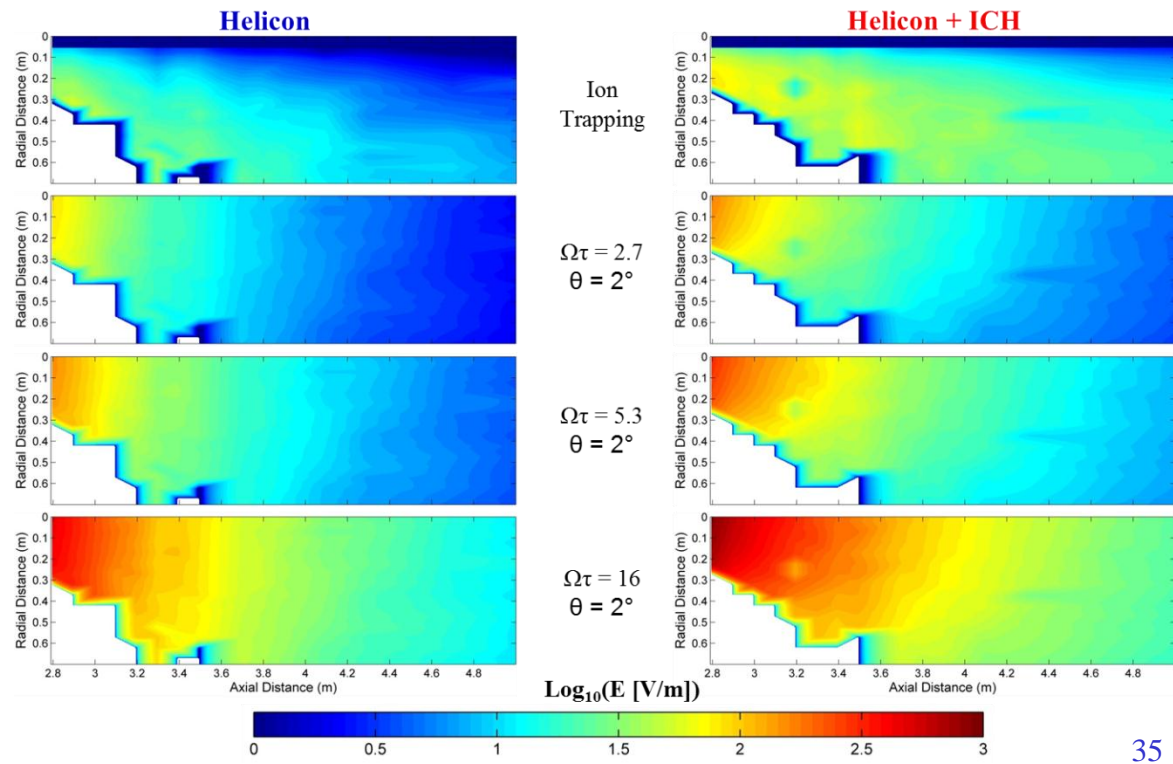
Ion trapping: Bound electrons trap free ions in the curved field.

$$\langle \tilde{E}_\perp \rangle_{IT} = \frac{m_i v_i^2}{q R_c}$$

Anomalous transport: Net electron transport inward drawn by the momentum of the ions.

$$\langle \tilde{E}_\perp \rangle_{AN} = v_i \sin \theta B \left[\frac{1 + \Omega_e^2 \tau_{eff}^2}{\Omega_e \tau_{eff}} \right]$$

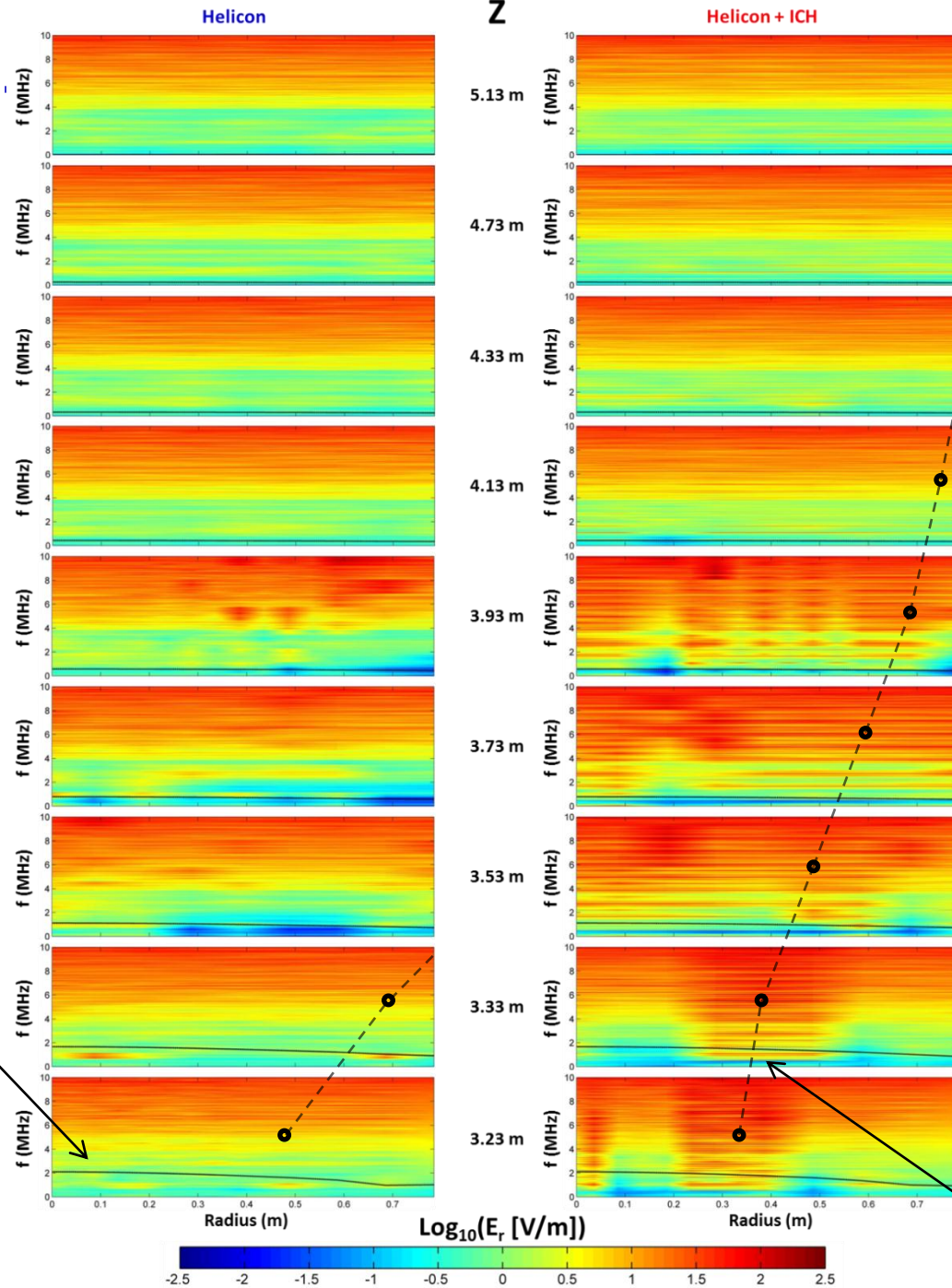
- Simulations of these competing electric forces indicates that there are regions in the plume where both *ion trapping* and *anomalous transport* will be more likely to dominate
- *Ion trapping* is most likely in the higher magnetic field regions and central plume where the radius of curvature (R_c) is large.
- *Anomalous transport* may occur further downstream in weaker magnetic field regions and along the edges of the plume
- The key is where are these fluctuating fields and what are the magnitudes?



There is an overall trend of increasing radial electric field strength at higher frequencies.

Unique to the case of hotter ions is that a distinct structure forms along the edge of the bulk flow.

Black Lines plot the lower hybrid frequency as a function of radius



The structure spreads and dissipates with increasing axial distance.

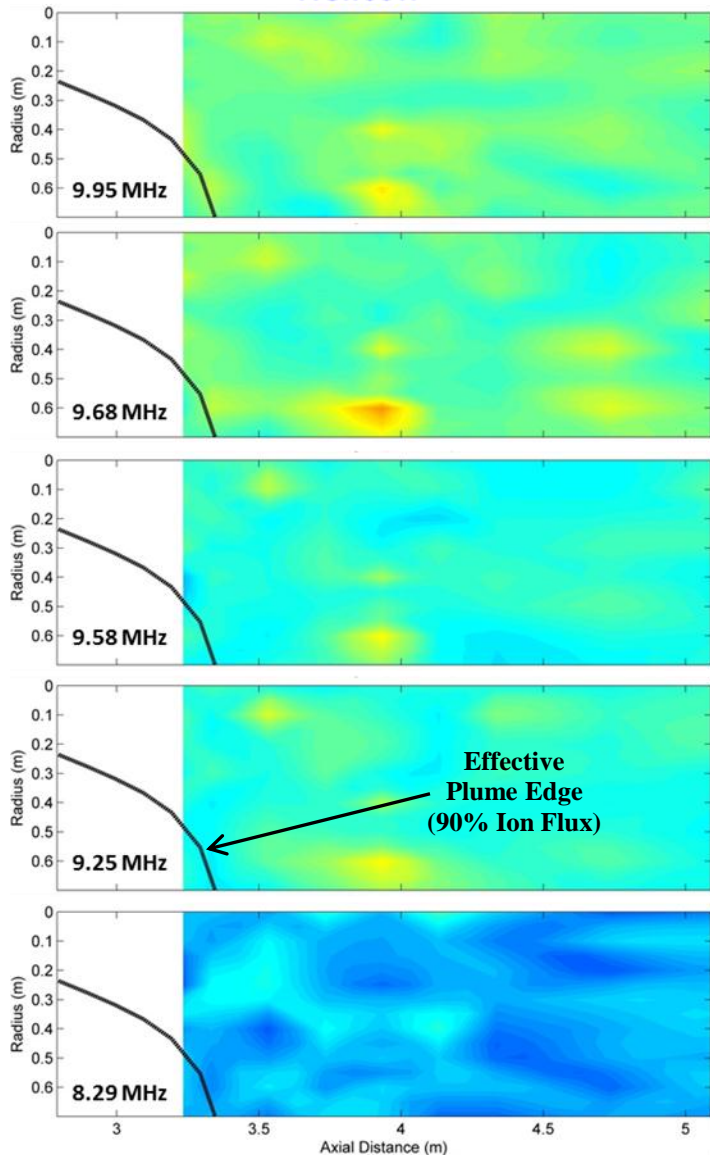
The location where this frequency dependent electric field ends is consistent with the location where the ions go to a linear/ballistic trajectory.

The structure of these peaks become more prominent plotting their magnitude as a function of (r, z) position...

Effective Plume Edge (90% Ion Flux)

$E_r(f)$ structure for 5 most prominent peaks

Helicon



The electric field during Helicon ($T_e \sim T_i$) lacks consistent structure

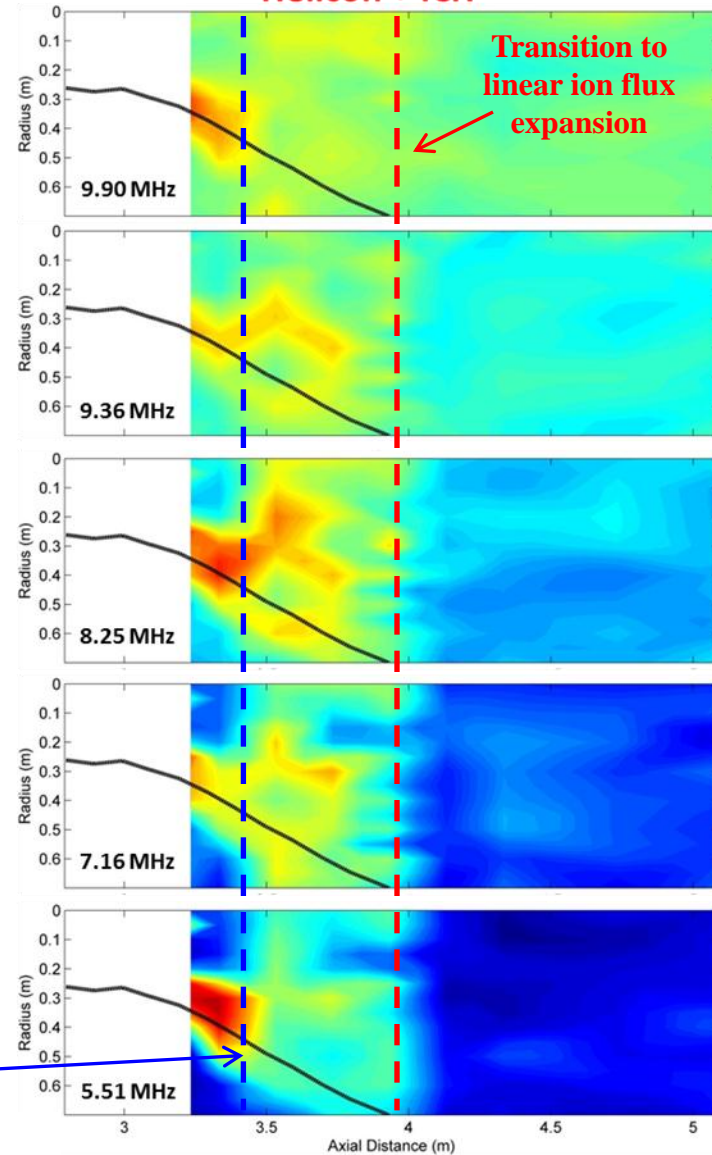
When ions are energized during ICH ($T_i \sim 5 - 7 T_e$) an organized structure is formed along the plume edge at several prominent frequencies.

The electric field magnitudes are consistent with regions of both ion trapping and anomalous transport and align with the ion flux data.

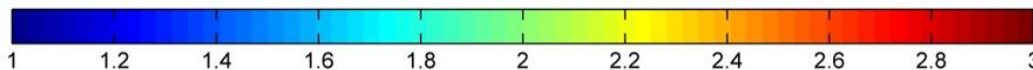
Anomalous electron transport values are estimated to be $\Omega\tau \sim 4 \pm 1$

Transition from ion trapping to anomalous transport

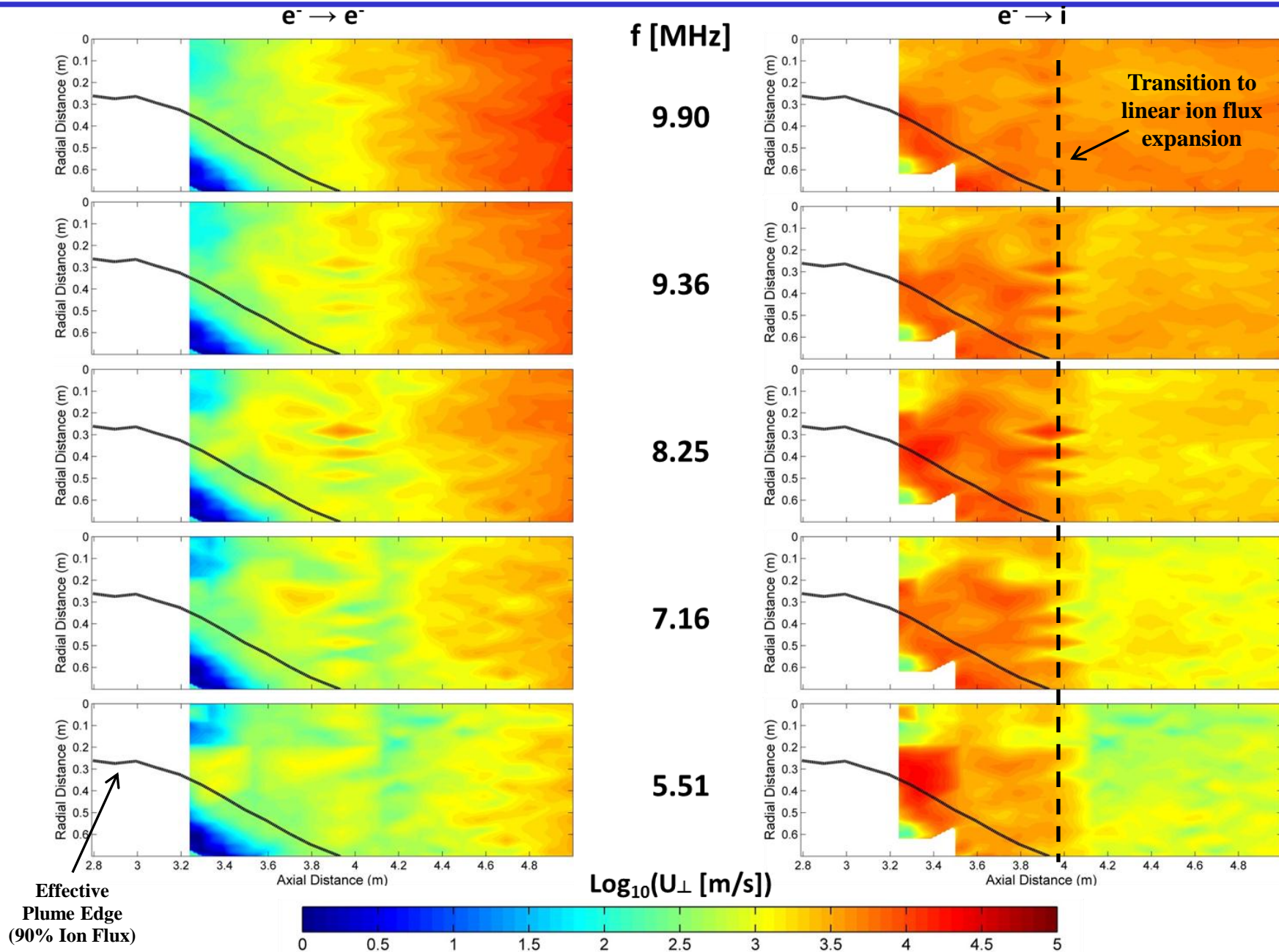
Helicon + ICH



$\text{Log}_{10}(E_r \text{ [V/m]})$



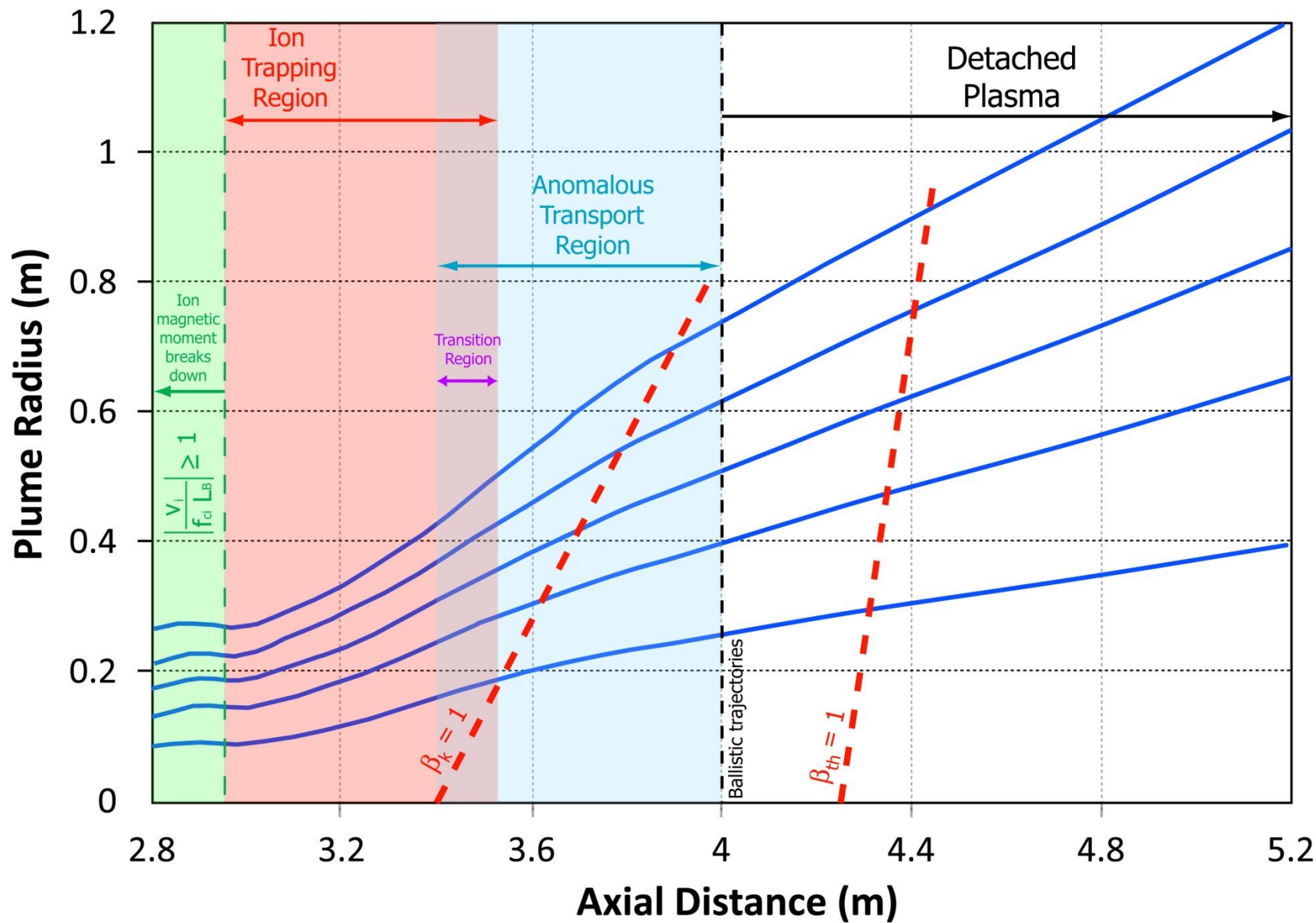
Net electron cross field velocity combining DC values with $E_r(f)$ largest peaks during ICH



Conclusions

- The plasma flowing through a dipole-expanding magnetic nozzle was mapped out using many traditional plasma diagnostics in a large vacuum chamber.
- Indications of a detached plume have been presented from multiple diagnostics showing the flow diverging from the magnetic field.
- These detachment trends have been compared to the leading published theories from the literature.
- The theories most consistent with the observed data are loss of adiabaticity (magnetic moment breakdown) and plasma turbulence.
- The detachment of the plume appears to be a two part process:
 - First, ions detach by magnetic moment breakdown creating a separation between ‘free’ ions and bound electrons.
 - Second, this separation causes instabilities to form (*LHDI?*) that drive anomalous resistivity along the edges allowing electrons to at first curve the ion trajectories before crossing the field lines to follow the ion momentum downstream.
 - Electrons detach further downstream by loss of magnetic moment (presumably).

The complete picture (during ICH)



Special thanks to the Ad Astra Rocket Company for funding this research

Thank You for listening to my talk

...questions?

Contact Information:
Christopher Olsen, Ph.D
chris.olsen@adastrarocket.com